Department of Environment Systems

Graduate School of Frontier Sciences

The University of Tokyo

2020

Master's Thesis

Spent coffee ground based adsorbent synthesis by hydrothermal carbonization
（水熱炭化によるコーヒー滓からの吸着剤合成）

Submitted August 27, 2020

Advisor: Associate Professor Teppei Nunoura
Co-advisor: Associate Professor Tomohiko Ihara

秦 世明
Shiming Qin

ACKNOWLEDGEMENTS

It is my pleasure to acknowledge the roles of the following individuals who had made a significant impact on my growth as a master student and who had helped me accomplish this master thesis.

First of all, I would wish to express my deepest gratitude to my supervisor associate Prof. Teppei Nunoura, who has offered me valuable suggestions in my academic studies. Especially in the COVID-19 lock down period, I was very upset about my study, Prof. Nunoura encouraged me to face a lot of difficulties.

Next, I would like to give my sincere gratitude to our lab's assistant professor, Dr. Osamu Sawai, for his valuable advice and patient guidance. He is always passionate on helping students who are in trouble.

I sincerely thank associate Prof. Tomohiko Ihara for his valuable comments on my research, which incented me to improve and widen my research from various perspectives.

I am extremely grateful to ISSP, The University of Tokyo, for providing their experimental equipment for me. I am hugely indebted to Prof. Daisuke Hamane, for helping on the SEM analysis in this thesis.

I would like to acknowledge Prof. Yoshihisa Asano of School of Engineering, The University of Tokyo, for helping in FT-IR analysis.

My sincere thank goes to the members of Nunoura Lab. Especially 2 doctor course students, Ms. Jennifer Chia and Ms. Diane Gubatanga, thank you for your valuable advices on my research work. I also want to thank Mr. Yiming Zhou, Mr. Takuya Ogawa, Mr. Tsuyoshi Kayamura, Ms. Xiaoyun Zhou, Ms. Jiongmei Yang, Mr. Peng Zhang, Ms. Yaru Wen, Ms. Dan Yang, thank you for your support on my research work and daily life.

Finally, I would like to dedicate this work to my parents for their unconditional love, support, believe and guidance, spiritual teachings and for everything that inspired me to achieve my goals in my personal life.

TABLE OF CONTENTS

1. Introduction

1.1 Introduction of coffee

1.1.1 Coffee and its market scale

Coffee is a brewed drink prepared from roasted coffee beans, the seeds of berries are from certain coffee species. It is darkly colored, bitter, slightly acidic and has a stimulating effect in humans, primarily due to caffeine content. [1] Coffee is one of the most popular drinks in the world. [2]

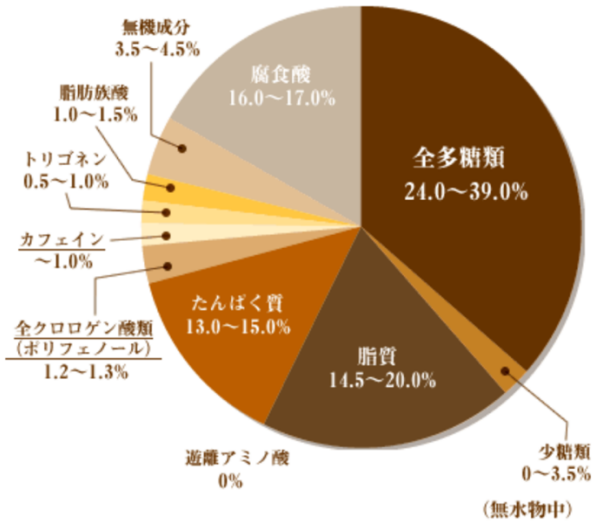

Figure 1-1 Constituents of dry coffee beans [5]

Coffee is a quite huge industry and has been widely consumed due to its refreshing properties [3]. According to the International Coffee Organization (ICO) [4], coffee bean production steadily increased from 5,586,120 tons in 1990 to 9,920,700 tons in 2018 in the whole world, while in Japan, it increased from 306,000 tons in 1990 to 468,000 tons in 2018. [5]

The constituents of dry coffee beans are shown in Figure 1-1.

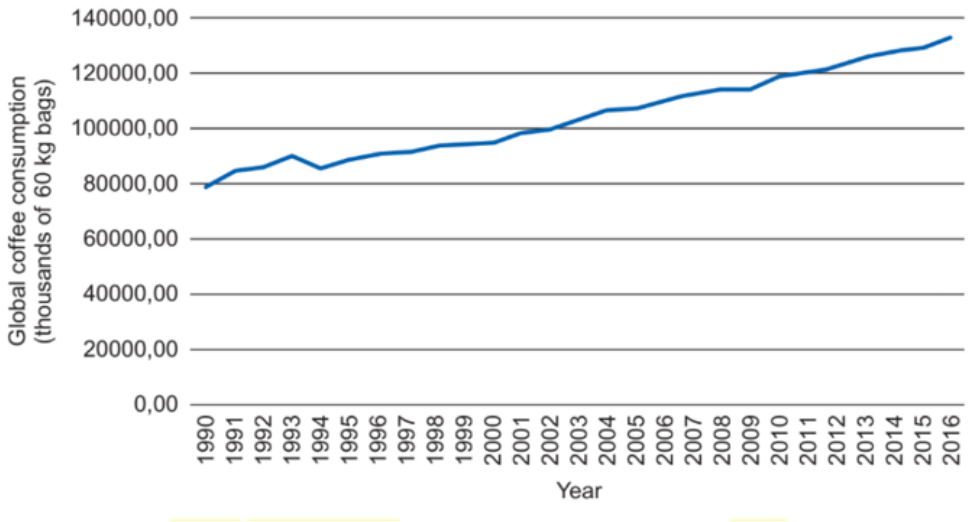

Figure 1-2 Global coffee consumption from 1990 to 2016[43]

1.1.2 Production process from coffee fruit to coffee beverage

Coffee production is the industrial process of converting the raw fruit of the coffee plant into the finished coffee. Once ripen, coffee berries are picked, processed, and dried. Dried coffee seeds (referred to as "beans") are roasted to varying degrees, depending on the desired flavor. Roasted beans are ground and then brewed with near-boiling water to produce the beverage known as coffee.

Picking

In the harvest season, the coffee fruit is removed by hand or machine. Whether picked by hand or by machine, all coffee is harvested in one of two ways: strip picking and selectively picking. Strip picking means removing all coffee fruit from the tree regardless of maturation state. This kind of picking can lower the labor cost as well as the flavor and odor. Another way, selectively picking means picking only the ripe coffee fruit individually. This kind of picking leads to labor-intense and thus cost more but can guarantee the fragrant, smooth, and mellow taste of coffee beverage.

Processing

The coffee berries are sorted by floating or winnowing to select good ripe fruit. And then the selected coffee berries are spread in the sun for about one month to dry to the optimum moisture content. The dried coffee berries are stocked in bulk until they are sent to mill.

Milling

The final steps before roasting is removing the last layers of dry skin and remaining fruit residue from the now-dry coffee, and cleaning and sorting it. These steps are often called dry milling to distinguish them from the steps that take place before drying, which collectively are called wet milling. [6]

Roasting

Coffee roasting is a complicated process that includes a number of physical and chemical transformations. The actual roasting begins when the temperature inside the bean reaches approximately 200 °C. Different varieties of seeds differ in moisture and density, therefore they are roasting at different rates. [7] During roasting, caramelization occurs as intense heat breaks down starches, changing them to simple sugars that begin to brown, which alters the color of the bean.

Coffee is usually served hot, although iced coffee is a popular alternative. Iced coffee is brewing by dark roast coffee beans while hot coffee is brewing by light roast coffee beans.

Grinding

The roasted coffee beans may be ground before brewing. The type of grind is often named after the brewing method for which it is generally used. Turkish grind is the finest grind, while coffee percolator or French press are the coarsest grinds. The most common grinds are between these two extremes: a medium grind is used in most home coffee-brewing machines. [8]

Brewing

Coffee ground must be brewed to create a beverage. Coffee may be brewed by several methods. It may be boiled, steeped, or pressurized. [9] Boiling is the fastest method, coffee ground is added to water and brought to the boil in a pot. Steeping combines that coffee ground and hot water in a vessel and left

to brew for a few minutes. Pressurizing forces hot pressurized and vaporized water through ground coffee. All of these methods have their merit and demerit and it depends on the type of coffee beverage. Spent coffee ground is separated after brewing and regarded as waste.

1.2 Significance of SCG (spent coffee ground) recycling

As told in 1.1.1, worldwide coffee bean production steadily increased from 5,586,120 tons in 1990 to 9,920,700 tons in 2018. It is estimated that 65% (w/w) of green coffee is converted to exhausted coffee grounds after soluble coffee production [10] so it can be speculated that about 6,500,000 tons coffee grounds are generated in coffee producing.

In fact, more than 90% SCG are dumped into general waste and sent to landfill where they emit carbon dioxide and methane, an important contributor because it has a global warming potential 28 times greater than that of CO_2 [44]. These greenhouse gases contribute a lot to global warming. Additionally, caffeine, an organic molecule largely consisting in coffee ground, can easily transfer into underground water. Since caffeine is toxic to birds and domestic animals, it can be a big threat to the ecosystem. Landfill of SCG also contributes towards the huge financial cost on tax payers of running and maintaining landfills.

1.3 Current technology to treat SCG

SCG can be used in many field, like compost, mushroom growth, biochar, bioactive compounds and anaerobic digestion as shown in Figure 1-3.

Compost

SCG have high nutrient levels, making them suitable for use in low-cost composting. Compost derived from coffee can be used to enhance soil nutrients and increase resistance against pathogens.

Mushroom growth

SCG can also be used as a growth medium for mushrooms. Mushrooms grown with coffee grounds boast the same nutrient quality as mushrooms cultivated on mediums currently being used by the mushroom industry, such as straw. The coffee brewing process sterilizes the coffee grounds, which is a vital process for the medium mushrooms grow on to remove contaminants.

Fuel production

Pyrolysis of SCG and generation of biochar is a very popular method to issue SCG waste problem in some developed countries nowadays. Pyrolysis is a process that thermally decomposes organic materials through the application of intense heat in the absence of oxygen. Without oxygen, the materials cannot combust and instead produce biogas, bio-oil and biochar.

Bioactive compounds

Coffee beans contain several classes of health-related chemicals, such as phenolic compounds, melanoidins, diterpenes, xanthines and vitamin precursors. As these compounds are only partially extracted during the brewing process, spent coffee grounds represent a potentially valuable source of bioactive compounds that have a wide range of applications in the food, cosmetic and pharmaceutical industries.

Anaerobic digestion

Anaerobic digestion is the process of breaking down organic material by microorganisms in the absence of oxygen. The output is a methane-rich biogas that can be used as a fuel and a nutrient-rich fertilizer. The biogas produced heats the building's water system and the digested products are available as a fertilizer.

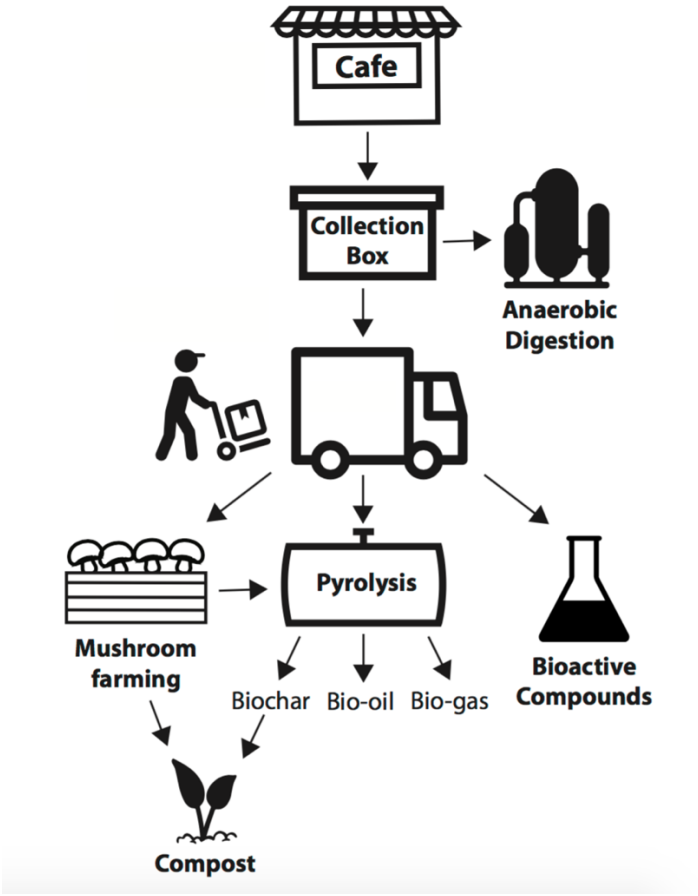

Figure 1-3 Current SCG recycling technology

1.4 Hydrothermal technology

1.4.1 Characteristics of hydrothermal technology

Hydrothermal technology is the technology utilizing high-temperature aqueous solutions at high vapor pressures. It could be divided into subcritical water (hot compressed water) and supercritical water based on the temperature and pressure.

The state of substance will change with temperature and pressure. Figure 1-4 shows the phase diagram of water. The critical point of water is 374 °C, 22.1 MPa. The water in the condition over the critical point is called supercritical water while the water near the critical point is called subcritical water or hot compressed water.

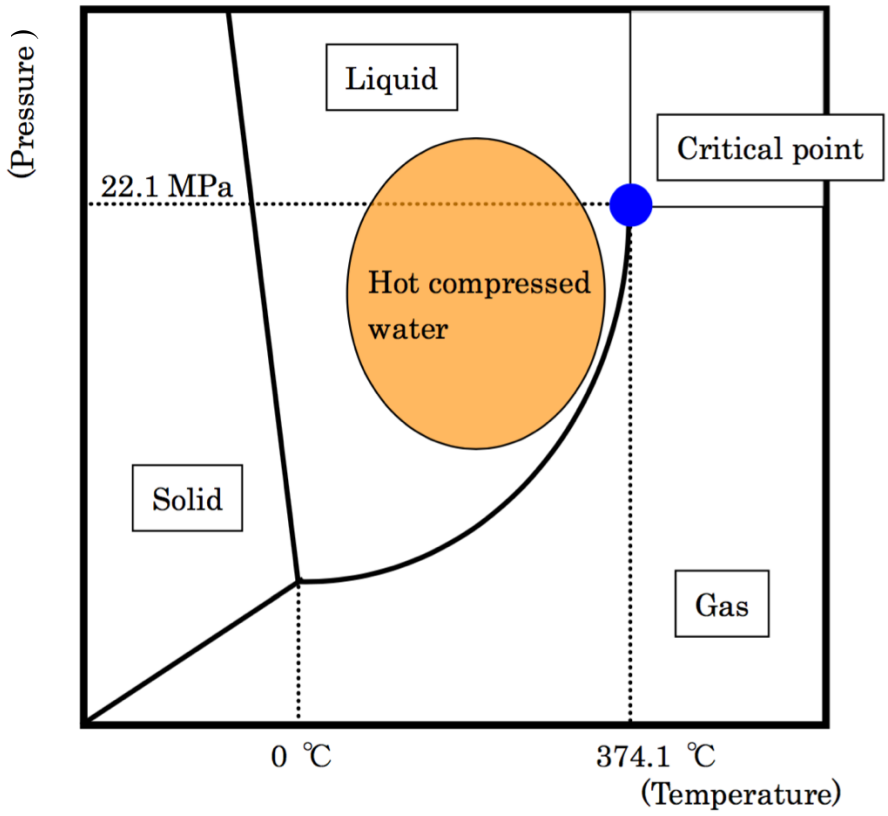

Figure 1-4 Phase diagram of water

The properties of subcritical water and supercritical water are quite different from that of normal water.

Figure 1-5 shows that over critical point of water, the dielectric constant of water decreases obviously. Higher dielectric constant means better dissolution capacity of polar substance (inorganic compounds) while lower dielectric constant means better dissolution capacity of nonpolar substance (organic compounds). Thus, compared with water in room temperature and pressure, sub and supercritical water could dissolve organic compounds easily while inorganic compounds will precipitate.

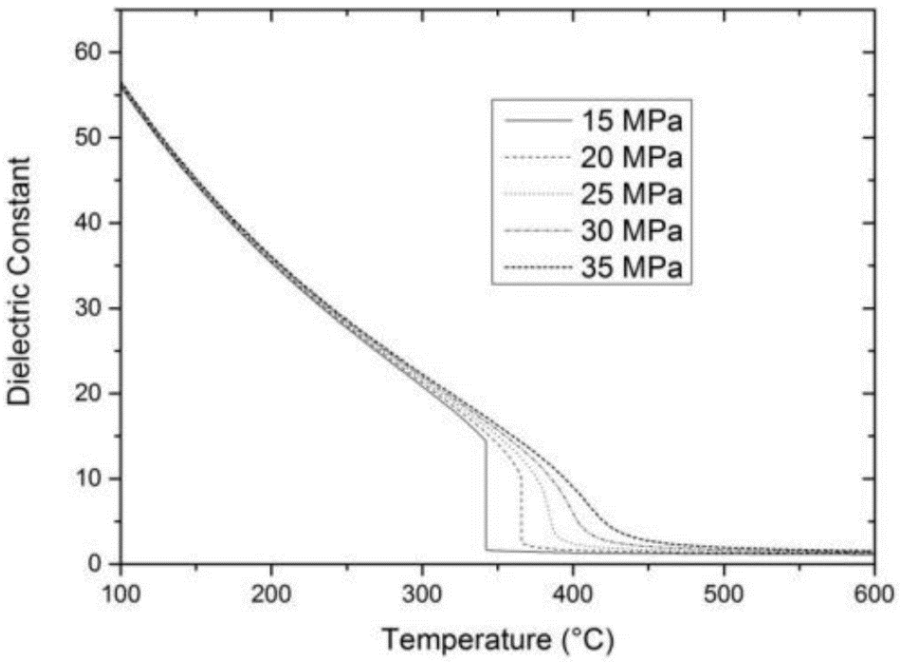

Figure. 1-5. Dielectric constant of water at various temperature and pressure [11]

Figure 1-6 shows ionic product of water increases with the rise of temperature and pressure, up to around 300 ℃ which means water dissociates into more H^+ and OH^-. In subcritical water, the concentrations of these two ions are about 30 times larger than that of water in room temperature. These ions are helpful to promote hydrolysis reaction [12].

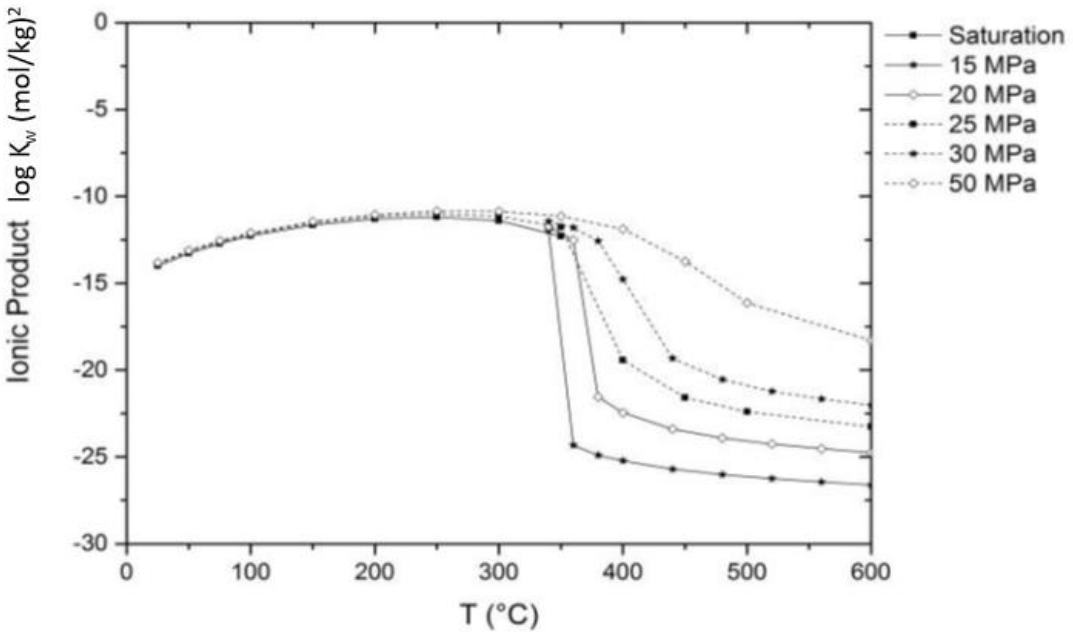

Figure. 1-6. Ionic product of water at various temperatures and pressure [13]

Thus, subcritical water and supercritical water could be utilized to dissolve organic compounds such as sewage sludge and plastic waste, and accelerate some reaction, such as carbonization.

1.4.2 Hydrothermal carbonization

Hydrothermal carbonization (HTC) is the treatment of organic matter in hot (150–350 ℃) water under autogenous pressure and residence times varying from minutes to hours. It simulates the natural formation of coal at lab scale. [14]

HTC is a technology specially designed for conversion of wet biomass feedstock with no dependency on energy input, which otherwise is needed for drying of the feedstock in other techniques. Pretreatment for drying of biomass is not needed in HTC, and it comprises three processes, namely, dehydration, decarboxylation, and decarbonylation.

The solid product is with a hydrophobic core and a hydrophilic shell containing large amount of OFGs (oxygenated functional groups). It is carbon-rich similar to lignite and can be easily pelletized. Figure 1-7 shows a hydrochar particles derived from cellulose. It is also known as hydrochar,

separated from the aqueous phase by a mechanical pressing process and has a higher heating value than that of the feedstock. It can be utilized as fuel, as an alternative for coal thus replacing a fossil fuel, as feedstock for gasification, as a soil additive for nutrient enrichment, or as an adsorbent or precursor for activated carbon [15].

Figure 1-8 shows the process of producing hydrochar through hydrothermal carbonization.

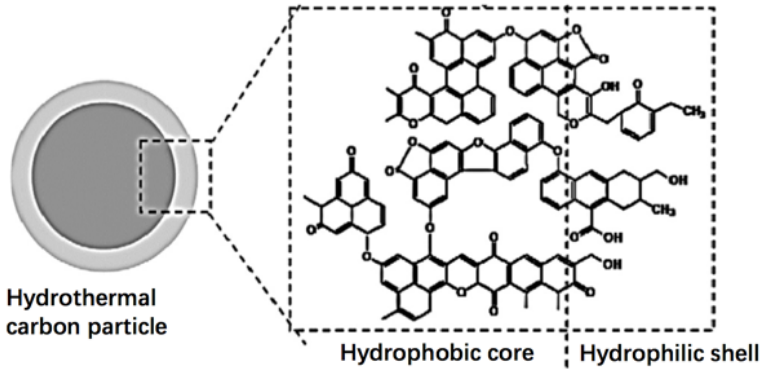

Figure. 1-7. Hydrochar particles derived from cellulose with hydrophobic core and hydrophilic shell [15]

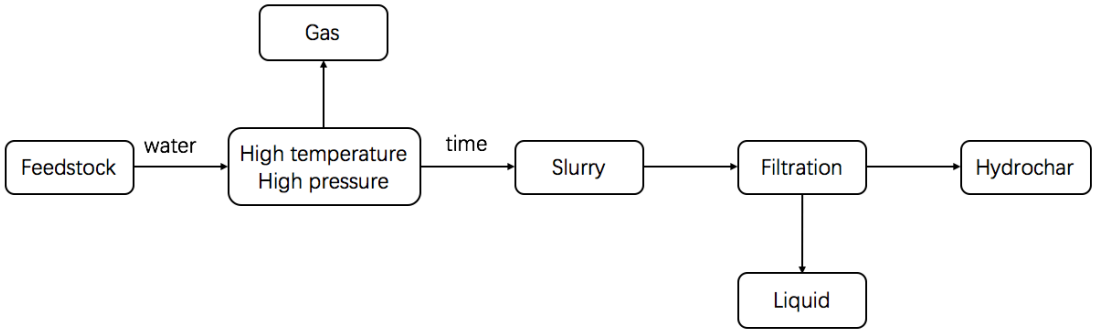

Figure. 1-8. The process of producing hydrochar through hydrothermal carbonization

1.5 Research purpose

This research aims to make out how applicable is hydrothermal method to produce adsorbent for wastewater treatment from SCG (spent coffee ground). In this research, batch type reactor is used to treat waste SCG by subcritical water. Through hydrothermal treatment, SCG hydrochar particles can be synthesized with a hydrophobic core and a hydrophilic shell containing large amount of OFGs (oxygenated functional groups). The presence of OFGs offers the advantage of further functionalization and makes hydrochar more hydrophilic for suitable applications including heavy metal and organic dye absorption. [16] This kind of carbonaceous material has a potential to be utilized in low contaminant concentration waste water treatment for their porosity has not been developed so that they can only achieve surface chemical absorption. Meanwhile for high contaminant concentration waste water treatment, further activation from hydrochar is necessary to synthesize activated carbon with strong adsorption capacity. OFGs content in hydrochar is an important factor which can decide the fate of porosity in the activated carbon. [17] And activated carbon with high porosity and high proportion of mesopore may be in favor of some kind of contaminant adsorption.

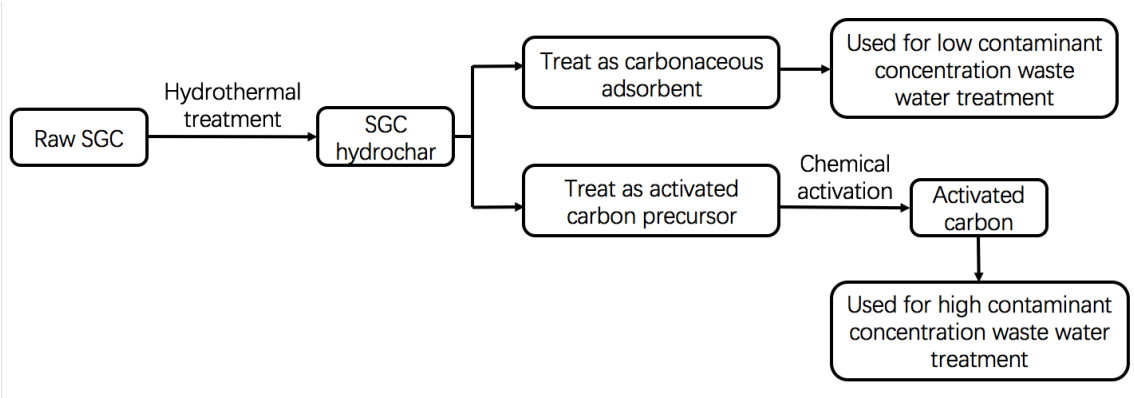

Figure. 1-9. Schematic diagram of this study

For treating SCG hydrochar synthesized via hydrothermal carbonization as a kind of carbonaceous adsorbent, objective of this section is to find a way to resolve research questions including:

a. What are the conditions in hydrothermal process needed for producing high performance carbonaceous adsorbent for heavy metal and organic dye contaminant in water solution?
b. What is the mechanism of carbonaceous adsorbent (SCG hydrochar) synthesized from SCG through hydrothermal process?
c. What is the main mechanism in the process of heavy metal and organic dye contaminant adsorption by this kind of carbonaceous adsorbent?

In order to resolve these problems, the following steps should be conducted:

a. Conduct carbonaceous adsorbent (SCG hydrochar) synthesis experiments in different reaction conditions (reaction time, temperature, amount of added H_2O, presence of oxidant additive) and test their production yield as well as heavy metal and organic dye adsorption ability by ICP-MS and UV-Vis, respectively.
b. Use FT-IR to analyze surface functional groups, and then use these analyses to give a clarification to the mechanism of hydrochar formation from SCG.
c. For the solid product (SCG hydrochar) applied as carbonaceous adsorbent, use Boehm titration method to determine their OFGs content, use BET method to measure their surface area, use SEM to observe their surface morphology. And then give a reasonable explanation of the relationship between the adsorption capacity and these factors as well as the adsorption mechanism.

For treating SCG hydrochar as a precursor in the activation process of activated carbon synthesis, objective of this section is to find a way to resolve research questions including:

a. What is the relationship between the precursor (SCG hydrochar) formation conditions (hydrothermal treatment conditions) and the activated carbon property after activation from the precursor?
b. What are the main influence factors of the precursor (SCG hydrochar) that attribute to adsorption capacity of activated carbon after activation from hydrochar?

In order to resolve these problems, the following steps should be conducted:

a. Conduct activated carbon synthesis through KOH chemical activation method from precursor (SCG hydrochar) and test their production yield and adsorption ability.
b. Use SEM to observe these activated carbon's morphology, use BET and BJH method to measure their surface area and pore size distribution and then use these analyses to give a reasonable explanation of different adsorption abilities among different SCG hydrochar derived activated carbon as well as heavy metal and organic dye adsorption ability by ICP-MS and UV-Vis, respectively.

1.6 Structure of the thesis

The thesis is composed of six chapters.

In Chapter 1, coffee, significance of SCG recycling, current treatment technology of treat SCG, hydrothermal technology, research purpose, scope and limitation of this study are introduced.

In Chapter 2, related literature is reviewed for deep understanding of hydrothermal carbonization of biomass.

In Chapter 3, research methodology, device and instruments are introduced.

In Chapter 4, synthesis of SCG hydrochar and SCG hydrochar derived activated carbon are reported. The characteristic analysis of hydrochar and activated carbon produced under different HTC operating conditions are investigated, and their synthesis reaction mechanism is also explained.

In Chapter 5, zinc ion and Rhodamine B dye adsorption performance by SCG hydrochar and SCG hydrochar derived activated carbon are evaluated, and the relationship between adsorption performance and HTC operating conditions are clarified.

In Chapter 6, research conclusions and recommendations are written.

In the end of the thesis, there is a list of reference.

1.7 Scope and limitation of this study

This study aims to develop a more efficient way to produce SCG based adsorbent material in order to realize the reduction of SCG landfilling and improvement of SCG material application.

This study was designed on a pilot scale, two batch setups, one for hydrothermal treatment and another for activation.

This study was limited to the use of SCG from cafeteria in Kashiwa Campus as a representative feedstock. Mixed SCG from Coffee beans for ice coffee and hot coffee in an approximate ratio of 3:7 (based on the consumption data in the recycling period) are used in all experiment. Furthermore, this study only used SCG derived from two brand of coffee beans, for ice coffee beans, Hills Bros (Japan), for hot coffee beans, UCC (USA).

The operating parameters of hydrothermal experiments in this study were effect of temperature, reaction time, water / SCG ratio and oxidant additives. All activation experiments were conducted at 600~650°C with hydrochar / KOH ratio in 1:3 and retention time of 1h.

The study was conducted at Environment Science Center, The University of Tokyo Kashiwa Campus. It was conducted under the supervision of Associate Professor Teppei Nunoura and Assistant Professor Osamu Sawai of Nunoura Laboratory.

2. Review of related literature

2.1 About hydrothermal conversion

2.1.1 Introduction of HTC

In the past few years, the use of hydrothermal carbonization (HTC) for conversion of biomass waste into carbonaceous materials has received considerable attention due to its ability to produce hydrochar for a variety of applications such as bio-energy, adsorption and activated carbon synthesis.

Basically, HTC is a thermo-chemical conversion technique which uses subcritical water for the conversion of wet biomass to carbonaceous products through fractionation of the feedstock. Carbonization temperature depends on the type of start material and its decomposition temperature. [18]

HTC involves several steps by hydrolysis of the biomass, forming smaller molecules, dehydration, and condensation or polymerization. The reaction conditions which are used in the HTC process are mild with temperatures from 180 to 250℃ and reaction times of several hours. The system pressure is autogenous, without the introduction of additional pressure. Long reaction times favor the formation of gaseous products and the amount of carbon derived from HTC decreases. On the other hand, the carbon energy density increases with increasing severity of the reaction conditions.

In turn, lignocellulosic biomass derived materials usually have a water content close to 40%. Traditional thermal processes include an initial pretreatment of the sample to reduce the water content. However, HTC process does not require such pretreatment. [19]

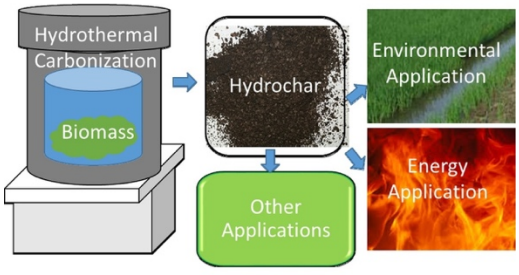

Figure. 2-1. Image of biomass waste life cycle through hydrothermal carbonization

Figure 2-1 shows the image of biomass waste life cycle through hydrothermal carbonization.

Kim et al. reported that the calorific value of exhausted coffee residue can be promoted to 26-27 MJ/kg through HTC under 210-240℃. [25] Zhao et al. published an article stating that food waste under hydrothermal treatment in the condition of 260℃, 4 hours and 80% moisture turned out a higher energy yield of 66.1%, and found that hydrochars added in the spent liquor could promote the specific methane yield, which was 2.53 times higher than no addition of hydrochars. [26]

Liu et al. used pine wood and rice husk to produce a kind of biochar for lead adsorption in aqueous solution, and found out the lead removal with capacities of 4.25 mg/g and 2.40 mg/g for pinewood and rice husk through hydrothermal treatment under operating temperature of 300℃ and reaction time of 5 hours. [27] Liu et al. has also done a comparison experiment between hydrochar under 300℃ and pyrolytic char under 700℃ from same kind of pinewood, although the BET area of pyrolytic char was higher than hydrothermal char, hydrochar's copper adsorption capacity was higher than pyrolytic char. It is inferred that ion-exchange reaction was the predominant removal mechanism in the case of hydrochar and its high oxygenated functional groups content contributed a lot for copper adsorption. [18]

Sevilla et al. used hydrothermally carbonized organic materials (furfural, glucose, starch, cellulose and eucalyptus sawdust) as precursor to produce activated carbon through KOH chemical activation. And a high surface area (up to 2700m^2/g) and a supermicropore range (0.7-2nm) material with narrow micropore size distribution was produced. The activated carbon materials exhibit high hydrogen uptakes, up to 6.4wt%, and large isosteric heats of adsorption, up to 8.5 kJ/mol. [28]

2.1.2 HTC of lignocellulosic biomass

During HTC, water acts like a kind of catalyst that facilitates hydrolysis and cleavage of lignocellulosic biomass; water possesses high ionization constant in hot compressed water zone (refer to Figure 1-6) and is responsible for hydrolysis of organics. [20] A decrease in pH during HTC of biomass is typically observed, which is due to formation of a variety of organic acids

such as acetic, levulinic, formic and lactic acids. The presence of these organic acids further promotes hydrolysis and decomposition of oligomers and monomers to smaller fragments. [21]

Hydrolysis can lead to a disintegration of the physical structure of biomass. With an increase in reaction severity, there is an increase in the amount of colloidal carbon particles. With an increase in process temperatures up to 220℃ and the autogenous pressure, most organics in biomass feedstocks are transformed into solids. [21]

As biomass comprises different polymer chains, the mechanism for the conversion to hydrochar is quite complex. Cellulose and lignin are considered to be the main constituents of typical biomass; Fig 2-2 shows the simplified version of the conversion of biomass to hydrochar.

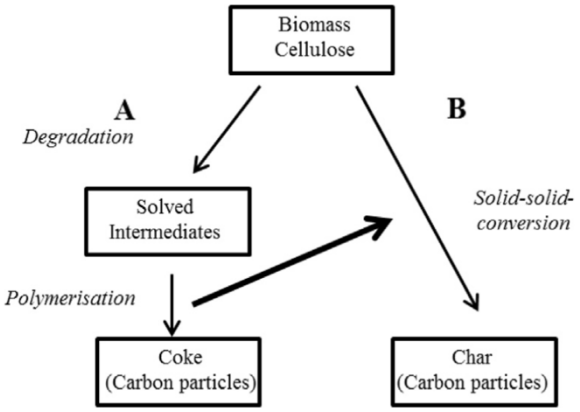

Figure. 2-2. Simplified version of the conversion of biomass to hydrochar [22]

Hemicellulose content in biomass partly undergoes hydrolysis at lower temperatures and results in the formation of hydrochar through polymerization (water solubility homogenous reaction). Kang et al. observed the hydrochar formation at 225℃ upon HTC of woodmeal mainly due to the hydrolysis of hemicellulose content [23].

Iryani et al. investigated the behavior of sugarcane bagasse through HTC using hot compressed water. He observed that when the temperature and reaction time was increased, hemicellulose and cellulose gradually dissolved, leaving a lignin-like acid insoluble residue. The presence of the residue increases the fixed carbon and decreases the volatile matter content of the solid product. [29]

Falco et al. reported the hydrochar formation from rye straw and the requirement of a high temperature for lignin decomposition. Lignin contributes to maintaining the natural macrostructure of the initial biomass into the final hydrothermal carbon products. Lignin interferes in the hydrolysis of cellulose and hemicellulose and slows the release of decomposition products formed from polysaccharides. [24]

Lignin present in biomass undergoes hydrolysis partly which leads to the production of phenolic hydrochar as in the case of pure lignin and might be linked to the polyaromatic char, non-dissolved lignin as shown in Figure 2-3. The hydrochar formed from polysaccharides and lignin contributes to the overall OFGs content in the hydrochar derived from biomass. At the same time, the OFGs content depends on the type of starting materials and the extent of reaction which is governed by a combination of temperature, time, substrate concentration and catalyst. The OFGs content in hydrochar is an important factor which can decide the fate of porosity in the activated carbon. [17]

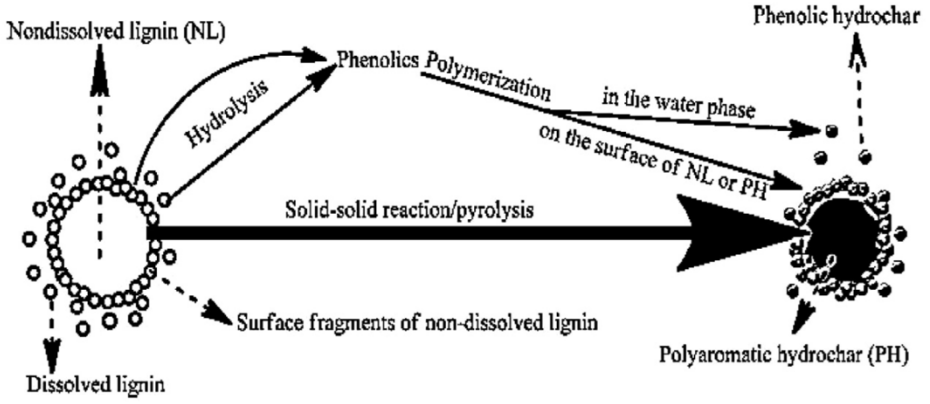

Figure. 2-3. Mechanism pathway for the formation of hydrochar from lignin [23]

2.1.3 Process parameters in HTC

Higher temperature leads to extensive dehydration and an increase in the degree of condensation of the hydrochar.

Sevilla et al. observed a decrease in the O/C and H/C ratios of cellulose with an increase in the temperature of HTC from 230 to 250℃. Cellulose that is hydrothermally treated at 220℃ shows FT-IR features containing C=O (carbonyl, carboxyl, quinone or ester) and OH. Whereas, cellulose hydrothermally treated at 210℃ does not undergo any chemical transformation and is found to have similar FT-IR features to those of the raw cellulose. [30]

Jain et al. investigated the effect of HTC temperature (200, 275, 315 and 350℃) on the formation of OFGs on coconut shell based hydrochars; it was observed that irrespective of temperature employed there was an increase in the OFGs content in hydrochar compared to raw shell. This increase can be attributed to the partial hydrolysis of polysaccharides and lignin present in the shell. A maximum in OFGs was observed at 275℃ followed by a decrease at 315 and 350℃. [31]

Residence time during HTC plays an important role in the extent of reaction and the distribution of different types of products and their quality.

He et al. reported a drop in OFG from 5.09 to 4.21 mmol/g as carbonization time increased from 4 hours to 12 hours. A peak in OFG is observed at 6 hours, followed by a decrease either due to (a) excessive dehydration or carbonization and formation of stable oxygen surface groups (ether or quinones) from OFGs or (b) its decomposition to gaseous products at longer residence time. [32]

Reduced concentrations of reactants in the hydrothermal environment minimize cross-reactions of the involved species and leads to a more defined product spectrum. On the other hand, at higher concentrations, it has been observed that there is negligible change in the production of liquid products and polymerization becomes a dominant process [33]. This is because the dissolved monomer units/decomposed products are more likely to undergo higher order (>1) polymerization (i.e. excessive aldol condensation and intermolecular dehydration) that converts liquid product to solid phase products. [34]

Sevilla et al. observed less condensed products (high O/C and H/C atomic ratios) at higher substrate concentrations due to incomplete hydrolysis. [30] Thus, substrate concentrations and residence times can be adjusted according to the product requirement and a higher concentration with a shorter residence time will be suitable for production of liquid phase products.

Numerous studies have been conducted with different catalysts for biomass decomposition under subcritical processing conditions of water either to enhance the reaction rate or to tailor the path of reaction for the desirable products. Increased decomposition in the presence of catalyst is attributed to the increased proton concentration leading to acid catalysis. Generally, small amounts of acids catalyze dehydration. [35]

Jain et al. reported that the hydrothermal pre-treatment of coconut shell in the presence of $ZnCl_2$ leads to hydrochar with high OFG content. Furthermore, by the use of H_2O_2, higher amounts of OFG were created on the hydrochar for efficient activation and higher porosity. [36]

2.1.4 Hydrochar applications

The hydrochar comprises condensed aromatic structures and bears high concentrations of OFGs. The presence of OFGs offers the advantage of further functionalization and makes hydrochar more hydrophilic for suitable applications including adsorption, catalysis, and as a precursor for activated carbon synthesis.

Liu et al. reported the formation of OFGs in the pinewood derived hydrochar which is found to be almost 340% higher compared to the pyrolytic char, and when employed as an adsorbent, it also showed 62% higher uptake of copper ions. The higher adsorption on hydrochar was attributed to the higher OFGs content since the porosity of pyrolytic char was comparatively higher. This demonstrates the importance of OFGs when it comes to involvement with cationic species. [18] Liu also demonstrated that pine-wood and rice husk derived hydrochars resulted in different OFGs content under the same processing conditions indicating the importance of origin of biomass. Pinewood hydrochar resulted in high content of OFGs and thus resulted in 77% higher removal of lead. [27]

Overall, in the absence of further processing, hydrothermal carbonization as a stand-alone process led to underdeveloped porosity. Thus, the direct use of hydrochar in various applications is not efficient compared to that of activated carbons with improved performance characteristics.

2.2 About activation

Activation is a process to change raw carbon material into porous material. Some suitable precursors such as lignocellulosic biomass can promote their performance as adsorbents after activation. High porosity is extremely desirable for enhanced performance of adsorbents since it facilitates high mass transfer fluxes and adsorbate loading.

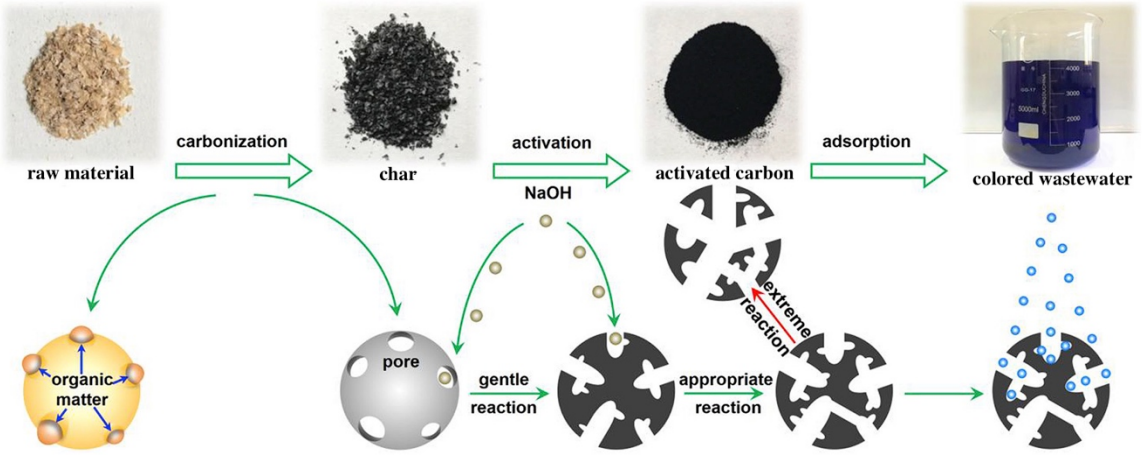

Figure. 2-4. The pathway of carbon material for adsorption from raw biomass [45]

Briefly, activation can be done in two ways, one is physical (or thermal) activation using CO_2 or steam at 800–900℃, the other one is chemical activation using KOH, $ZnCl_2$, H_3PO_4, etc. typically in the range of 450–650℃.

In addition, chemical characteristics of the lignocellulosic biomass are of significance and play a substantial role in creation of porosity in activated carbons. Therefore, it is of great importance to understand the role of these characteristics in development of porosity in carbons and thus optimize the process conditions by the use of appropriate pre-treatment processes.

Falco et al. demonstrated how the temperature of hydrothermal process affects the derived activated carbons from KOH activation. Extent of

carbonization, aromatization and carbonyl functionalities are reported to increase up till 240℃which led to an increase in porosity in activated carbons. A further increase in temperature to 280℃led to enhanced chemical stability and structural order in the precursor which led to the decline of porosity in the derived carbons. [37]

Romero-Anaya et al. investigated the effects of various chemical activating agents (KOH, NaOH and H_3PO_4) and the physical activating agent, CO_2, on porosity creation with glucose and sucrose derived hydrochars as precursors. The BET surface areas obtained were nearly 3100 m^2/g with KOH:precursor ratio of 4:1 and 5:1 for glucose and sucrose derived hydrochars, respectively, indicating the role of the starting material in the formation of porosity. [38]

Reactivity of precursors or the OFGs content in the precursor is an important indicator of the effectiveness of chemical activation and can thus predict the extent to which porosity will be developed in the activated carbons. [28]

Liu et al. reported the use of rice husk and pinewood derived hydrochars as the precursors for the activated carbon synthesis via physical activation using CO_2. The BET surface areas obtained are 569 m^2/g and 446 m^2/g for pinewood and rice husk hydrochars derived carbons, respectively. The OFGs content in the pinewood derived hydrochar was higher which might have resulted in higher surface area. [39]

3. Methodology

3.1 Preparation of spent coffee ground

In this research, spent coffee ground (SCG) was collected from caféteria in Kashiwa Campus. There are two kinds of coffee beverage supplied in that cafeteria, ice coffee (Hills Bros Bali Arabica blend) and hot coffee (UCC Café Nature). These two kinds of coffee beans are used as feedstock to make coffee in that caféteria (see Figure 3-1), thus the coffee ground collected from coffee-maker in the caféteria were also mixed coffee ground. Based on the consumption data of that month (November 2019), the ratio between ice coffee and hot coffee can be speculated to be 3:7.

Figure 3-1 Ice coffee beans and hot coffee beans used in the caféteria

These SCG were well mixed and then put into a steel pot and dried in an oven at 105°C overnight as shown in Figure 3-2. After that, these SCG were sealed in a plastic bag and stocked in a dry box for following experiments as shown in Figure 3-3.

Figure 3-2 Raw spent coffee ground material after drying

Figure 3-3 Raw spent coffee ground material sealing in a plastic bag

3.2 SCG hydrochar synthesis experiment

3.2.1 Batch-type reactor

In the SCG hydrothermal carbonization experiment of this research, a batch type reactor was used. This synthesis reactor is a tube made of SUS316 containing chromium (16% -18%), nickel (10% -12%) and molybdenum (2%-3%) (Ohmiya & Fujii, 2012). This type of stainless steel was selected because it was resistant to acid and high-temperature corrosion.

Figure 3-4 is the hydrothermal synthesis reactor. The gas collecting reactor was designed as shown in Figure 3-5. Different from the synthesis reactor, one side of the gas collecting reactor was connected with a 1/2 inch into 1/8 inch reducer. Then, it was connected to a 20 cm, 1/8 inch tube, the other side of this 1/8 inch tube is connected to a sampling valve.

The total volume of the reactor is 23.3 mL. The maximum use pressure of the reactor is 28.9 MPa below 93℃and 22.83 MPa in 426℃.

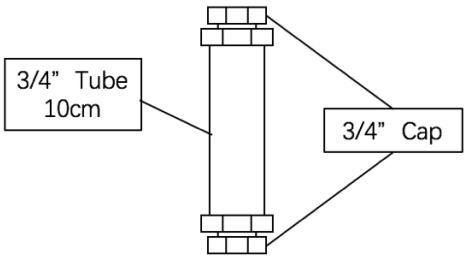

Figure 3-4 The schematic diagram of the hydrothermal synthesis reactor

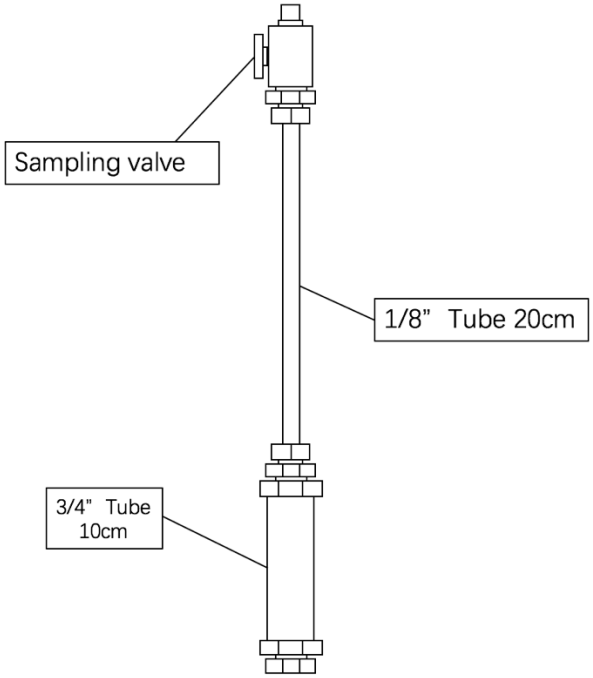

Figure 3-5 The schematic diagram of gas collecting reactor

3.2.2 Salt bath device

Salt bath device was selected as the heating method for this experiment because it has two advantages compared to electric or gas furnace method: (1) molten salt has better thermal conductivity and can heat up the reactor more uniformly (with uniform thermal conduction); (2) the reactor can be put into salt bath when reaching experimental temperature, which could avoid the occurrence of side reactions during heating up. The salt bath device consists of a molten salt bath, thermocouple and air pump (Figure 3-6). Molten salt was composed of KNO_3 (53%), $NaNO_2$ (40%) and $NaNO_3$ (7%), mixed in the bath as the heat transfer medium. Because the melting point of this type of molten salt was around 142 ℃ to 148 ℃ and boiling point was 680 ℃, the temperature controlled by the salt bath device was in the range of 150 ℃ to 600 ℃, which was suitable for this experimental temperature (180 ℃ to 300℃). The temperature of molten salt was monitored and controlled by a T-35 type K sheath thermocouple (produced by SAKAGUCHI VOC CORP.). In

addition, an air pump was used in this device to blow air into the molten salt to ensure the temperature to be distributed evenly in the salt bath. The temperature of the salt bath was also monitored by the SD16A21-05 indicator (produced by SHIMADEN CO. LTD.).

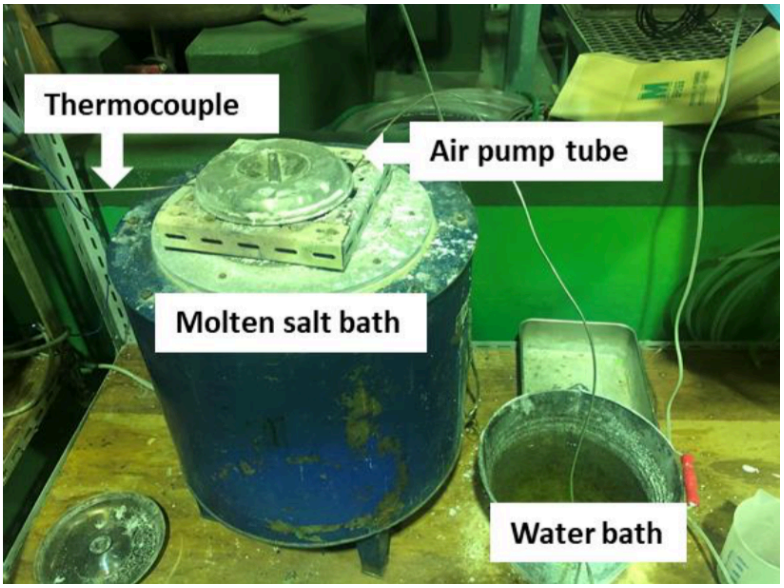

Figure 3-6 Photograph of the salt bath device.

3.2.3 Experiment conditions

All the experimental conditions are summarized as followings

a. Temperature

Table 3-1. Experimental conditions based on temperature variables

No.	Temperature	Reaction time	H_2O/SCG ratio	Presence of HNO_3
1	180℃	2h	2:1	0%
2	210℃			
3	240℃			
4	270℃			
5	300℃			

b. Reaction time

Table 3-2. Experimental conditions based on reaction time variables

No.	Temperature	Reaction time	H_2O/SCG ratio	Presence of HNO_3
1	180℃	2h	2:1	0%
2		4h		
3	240℃	2h		
4		4h		
5	300℃	2h		
6		4h		

c. H_2O/SCG ratio

Table 3-3. Experimental conditions based on water volume variables

No.	Temperature	Reaction time	H_2O/SCG ratio	Presence of HNO_3
1	180℃	2h	2:1	0%
2			5:1	
3	240℃		2:1	
4			5:1	
5	300℃		2:1	
6			5:1	

d. Presence of HNO_3

Table 3-4. Experimental conditions based on HNO3 additive variables

No.	Temperature	Reaction time	H_2O/SCG ratio	Presence of HNO_3
1	180℃	2h	2:1	0%
2	240℃	2h		
3	300℃	2h		
4	180℃	2h		100%
5	240℃	2h		
6	300℃	2h		

3.2.4 Experiment procedure

Deionized water and SCG from the stock bag were mixed in a certain ratio as shown in Table 3-5. These starting materials were prepared in the reactor shown in Figure 3-4 and Figure 3-5. The reaction was initiated by immersing the reactor into the molten salt bath. After a predefined period, the reactor was quenched by water to room temperature to stop the reaction. (Figure3-7) The solid product, which was called hydrochar, was separated by suction filtration followed by drying in an oven at 105℃overnight.

Table 3-5. Actual feedstock weight and water volume of different H2O/SCG ratio

H_2O/SCG ratio	Volume of water (mL)	Weight of SCG (g)
2:1	8	4
5:1	5	1

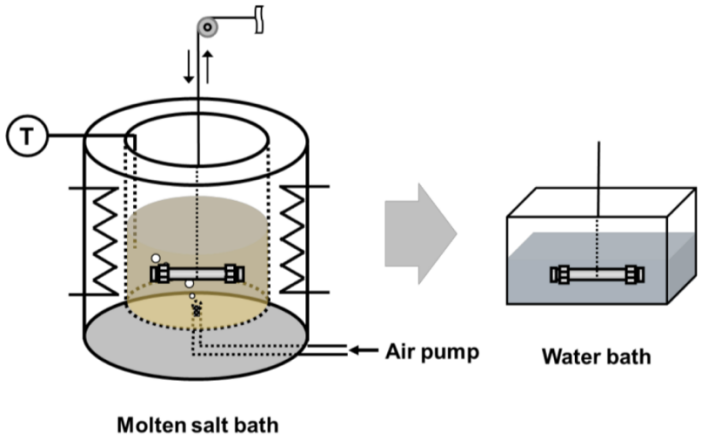

Figure 3-7 Schematic diagram of hydrothermal treatment experimental procedure

After dried, these hydrochar sample was collected in a reagent bottle for following analysis and adsorption experiment.

3.3 SCG hydrochar activation experiment

3.3.1 Tube furnace activation set-up

The tube furnace activation set-up consists of nitrogen supply system, quartz tube, ceramic boat and tube furnace as shown in Figure 3-8.

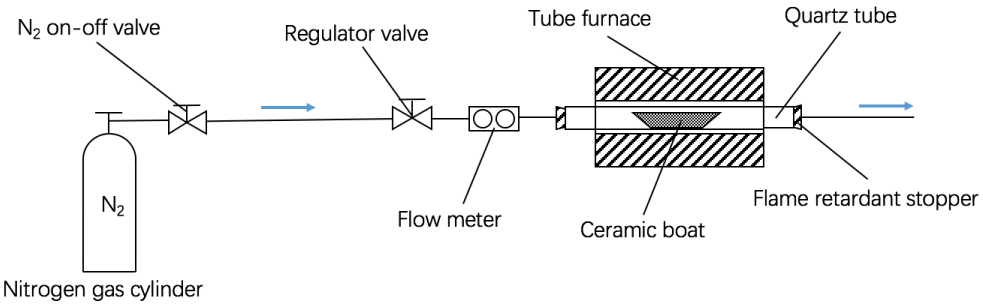

Figure 3-8 Schematic diagram of tube furnace activation set-up

3.3.2 Samples for activation

Hydrochar obtained under the HTC conditions listed in the following table were used as samples for activation experiment.

Table 3-6. Experimental conditions for obtaining hydrochar samples for activation test

No.	Temperature	reaction time	H_2O/SCG ratio	Presence of HNO_3
1	180℃	2h	2:1	0%
2	240℃			
3	300℃			
4	180℃			5%
5	240℃			
6	300℃			

3.3.3 Experiment procedure

Hydrochar was thoroughly mixed with KOH in the ratio of 1:3 (2 gram hydrochar and 6 gram KOH powder). The mixture was then heat treated to

the target temperature 600℃ (heating ramp rate in 4℃/min) in a tube furnace under a nitrogen gas flow (400 mL/min) and held at the target temperature 600℃ for 1 h.

After designated reaction time, the cover of tube furnace was opened to let the temperature cool down soon to stop the activation reaction. Meanwhile N_2 was kept flowing during the cooling time. After the reactor had been totally cooled down, the activated samples were taken out and then thoroughly washed several times with 10 wt% HCl to remove any inorganic salts, and then washed with distilled water until neutral pH. Finally, the activated carbon was dried in an oven at 105℃ overnight and collected in a reagent bottle for following analysis and adsorption experiment.

3.4 Adsorption experiment

3.4.1 Magnetic stirring device

Magnetic stirring device (Figure 3-9) was used in both RhB and zinc ion adsorption experiment. Through stirring, the liquid phase turbulence is accelerated, and the adsorbent is fully contacted with the solutes, which contributes to mass transfer, so it can effectively improve the adsorption efficiency and facilitates the adsorption process.

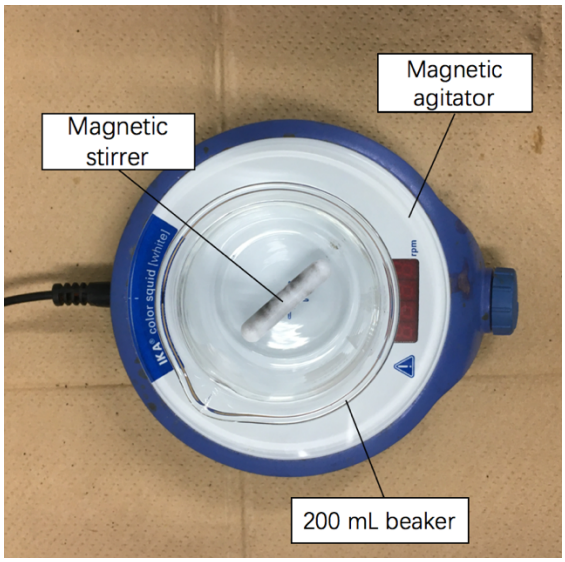

Figure 3-9 Photograph of magnetic stirring device

3.4.2 Centrifuge

As shown in Figure 3-10, a table top centrifuge (KUBOTA 2420) was used to separate solid (adsorbent) and liquid after agitation in predefined time.

After adsorption experiment, about 10 mL of the solution mixed with adsorbent was sampled after agitation and filled in glass test tube. And then these glass test tubes were put into the centrifuge. Note that tubes must be put along the diagonal to avoid mechanical trouble. The rotation speed is 3000rpm, and rotation time is 1min.

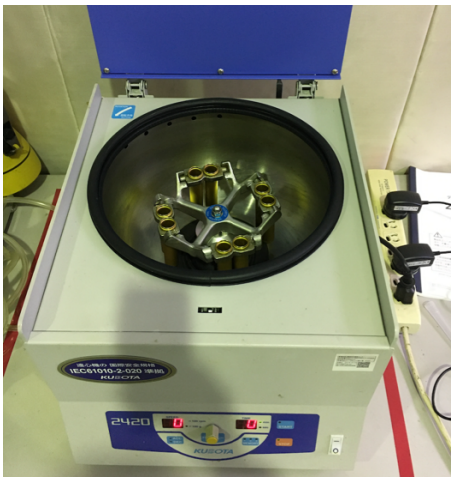

Figure 3-10 Photograph of centrifuge with the cover opened

3.4.3 Ultraviolet-visible (UV-vis) spectrophotometer

UV-vis spectroscopy refers to absorption spectroscopy or reflectance spectroscopy in part of the ultraviolet and the full, adjacent visible spectral regions. This means it uses light in the visible and adjacent ranges.

In this research, UV-Vis spectrophotometer is used to determine Rhodamine B (RhB) concentration. In this experiment, UV-1650PC (SHIMADZU Corporation) was used.

The procedure of UV-vis spectroscopy analysis is listed as followings:

a) A calibration curve for RhB's peak absorbance is plotted first so that the range of adsorption spectrum and corresponding RhB

concentration can be defined. In all analyses, UV-vis quartz glass cells were washed more than once between measurements.

b) Draw a baseline with deionized water.

c) Analyze the solution sample. Set the cell of deionized water into the farther slot and set the cell of sample solution into the closer slot.

d) If the absorbance of the sample is higher that the range of calibration curve range, dilution is needed to make sure that the absorbance is in the range of calibration curve range to keep the accuracy of concentration.

3.4.4 ICP-MS

Inductively Coupled Plasma Mass Spectrometry (ICP-MS) was used to analyze Zn^{2+} concentrations in liquid sample. The instrument is ICPM8500 produced by SHIMADZU Corporation.

Tuning solution is made of Lithium, Bismuth and Indium standard solution. After tuning, in order to make a Zn^{2+} calibration line, 500ppm Zn^{2+} standard solution was used. This kind of Zn^{2+} standard solution was made by $Zn(NO_3)_2 \cdot 6H_2O$ (FUJIFILM Wako Pure Chemical Corporation). 0.5ppm, 0.25ppm, 0.1ppm of Zn^{2+} solution was used to make a calibration line of concentration with intensity. The concentration of samples has to be in the range of 0.1-0.5ppm, or it should be adjusted to keep the accuracy. At least 10 mL of each sample injection was prepared to make sure that enough sample was available for rinsing and analysis.

The procedure of ICP-MS analysis is listed as followings:

a) Draw the calibration line.

b) Dilute liquid sample and analyze it by ICP-MS.

c) Calculate the metal concentration in liquid sample

3.5 Analytical method

3.5.1 Proximate analysis

Proximate analysis is formally defined by a group of ASTM test methods and is an assay of the moisture, volatile matter, fixed carbon, and ash content of a coal sample.

In this study, it was used to determine the carbonization extent of hydrochar products. As samples are all dried in an oven as shown in Figure 3-11, only volatile matter, fixed carbon, and ash content are measured.

The procedure of proximate analysis is listed as followings:

a) About 1 g finely powered dry sample is weighed in a silica crucible. (Attention should be paid because the silica crucible is very fragile)

b) The crucible is covered with a lid and placed in a muffle furnace as shown in Figure 3-11 maintained at 925±20℃ for 7 min.

c) The crucible is cooled in air, then in a desiccator and weighed again, where loss in weight at 925±20℃ is the weight of volatile matter.

d) The residue sample in the crucible is then heated without lid in a muffle furnace at 700±50℃ for 30 min.

e) The crucible is then taken out, cooled first in air, then in a desiccator and weighed. The residue weight of sample is reported as ash weight and the loss in weight at 700±50℃ is the weight of fixed carbon.

f) Finally calculate their percentage content by dividing by the weight of initial weight of dry sample.

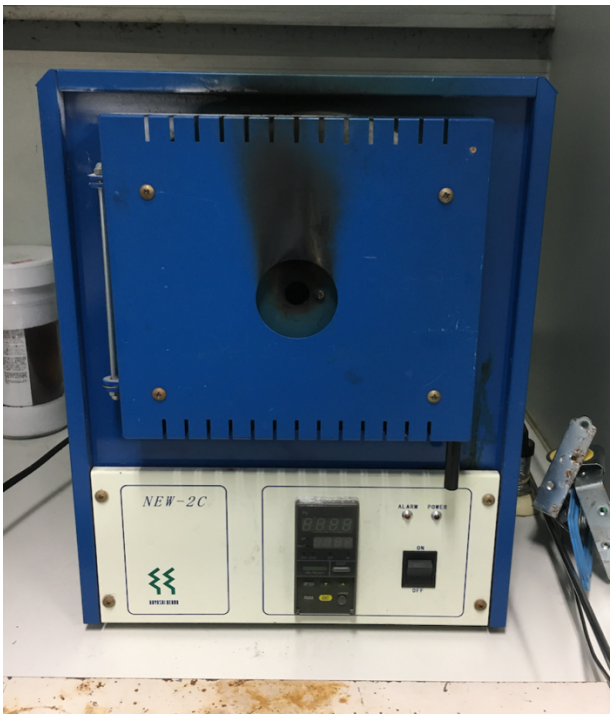

Figure 3-11 Photograph of muffle furnace

3.5.2 SEM analysis

A scanning electron microscope model, JSM 5600 (JEOL) was used to observe the hydrochar and hydrochar derived activated carbon sample's surface in the electron microscope section, ISSP, the University of Tokyo. The samples in powdered form were attached on a double-sided adhesive carbon tape and mounted on a silver sample holder. Moving the holder and adjusting the focus to search for ideal image of samples and save them in the computer.

3.5.3 BET/BJH analysis

3.5.3.1 BET analysis

This technique was used to measure the specific surface area of the activated carbon. This technique is based on the well-known Brunauer, Emmett and Teller (BET) [40] theory which is used to estimate the number of

molecules required to cover the adsorbent surface with a monolayer of adsorbed molecules. Nitrogen is usually employed as the gaseous adsorbate for this analysis. Consequently, standard BET analysis is usually conducted at the boiling temperature of N_2 (-196.15 ℃or 77 K). The range of validity of this theory is between 0.05 and 0.35 relative pressure. The BET equation is given by Equation 3-1.

$$\frac{1}{v(\frac{P_0}{P}-1)} = \frac{c-1}{v_m\, c}(\frac{P}{P_0}) + \frac{1}{v_m\, c} \qquad 3\text{-}1$$

where: P = equilibrium pressure

P_0 = saturation pressure

v = adsorbed gas quantity

v_m = monolayer adsorbed gas quantity

c = BET constant

The total surface area (S_{total}) and the specific surface area (S_{BET}) are given by:

$$s_{total} = \frac{(v_m\, N\, s)}{V} \qquad 3\text{-}2$$

$$s_{BET} = \frac{S_{total}}{\alpha} \qquad 3\text{-}3$$

where: N = Avogadro's number

s = adsorption cross section of the adsorbing species

V = molar volume of the adsorbate gas

α = mass of adsorbent

The pore diameter can be computed from the results of BET analysis. The total amount of N_2 taken up at a pressure of 1 atm and at a temperature of 77 K gives the total pore volume (V_{pore} or v). With the model of cylindrical pores the total pore volume is:

$$V_{pore} = \frac{1}{4}\,\pi\, d^2\, L \qquad 3\text{-}4$$

where: d = mean pore diameter

L = total length of pores

Rearranging equations 3-2 to 3-4, other parameters such as pore diameter and pore length were determined.

3.5.3.2 BJH analysis

The method developed by Barrett, Joyner, and Halenda is a procedure for calculating pore size distributions from experimental isotherms using the Kelvin model of pore filling. From the isotherms, the number of micro, mesopores and macropores is determined. This technique is done with the continued addition of gas molecules beyond monolayer formation. This eventually leads to the gradual stacking of multiple layers (or multilayers). The range of validity of this theory is between 0.35 and 0.99 relative pressure. Their formation occurs in parallel to capillary condensation. The latter process is approximated by the Kelvin equation, which quantifies the proportionality between residual (or equilibrium) gas pressure and the size of capillaries capable of condensing gas within them. To investigate the way liquid N_2 is condensed or evaporated during the adsorption and desorption

3-5

cycles, the pressure at which the liquid will condense in a radius, r_k is given by the Kelvin Equation:

$$In\left(P/P_0\right) = \frac{-2\,\gamma\,V_m\,cos\emptyset}{R\,T\,r_k}$$

where: r_k = Kelvin radius or critical radius

γ = surface tension of the condensed liquid

$\emptyset$ = equilibrium contact angle (usually assumed to be 0° due to complete wetting)

Taking into account the statistical film thickness change after each decrement of P/P_0 , an equation developed by de Boer [40] for the estimation of film thickness is as follows:

$$t\,(Å) = \left(\frac{13.99}{\log\left(P_o/P\right) + 0.034}\right)^{\frac{1}{2}} \qquad 3\text{-}6$$

Then, the pore radius is given by:

$$r_p = r_k + t \qquad 3\text{-}7$$

3.5.3.3 Sample preparation and analysis procedure

Quantachrome Nova 2000e surface area and pore size analyzer was used to measure surface area and pore-related parameters by BET and BJH method. Before each gas sorption analysis, the sample was degassed to completely clean the catalyst surface by flowing an inert gas (N_2) under high vacuum conditions. Table 3-7 presents the conditions for BET and BJH analysis.

Table 3-7 Parameter conditions for BET and BJH analysis.

Parameter		Analysis	
		BET	BJH
Gas sorption system		NOVA 2000e (QUANTACHROME)	
Adsorbate		Liquid N_2	
Adsorbate cross section ($Å^2$)		16.2	
Outgas time (min)		60	
Outgas temperature (℃)		300	
Isotherms	Adsorption	✔	✔
	Desorption	-	✔
Parameters	Surface Area ($m^2\ g^{-1}$)	✔	-
	Particle density ($g\ cm^{-3}$)	-	✔
	Pore volume ($cm^3\ g^{-1}$)	-	✔
	Pore diameter (Å)	-	✔
	Particle length (Å)	-	✔
Approx. total analysis time (min)		80	280

3.5.4 Boehm titration method

The Boehm titration (BT) is a method that enables a quantification of specific surface oxygenated functional groups on carbon materials. It provides absolute values based on a chemical reaction. The quantification of the reactions is realized by titration.

The Boehm titration works on the principle that oxygen groups on carbon surfaces have different acidities and can be neutralized by bases of different strengths. Sodium ethoxide ($NaOC_2H_5$), sodium hydroxide (NaOH), sodium carbonate (Na_2CO_3) and sodium bicarbonate ($NaHCO_3$) are the four bases used in this titration. They are regarded as approximate probes of a distribution of oxygen surface groups according to the scheme: $NaHCO_3$ (carboxyl), Na_2CO_3 (carboxyl and lactonic), NaOH (carboxyl, lactonic and phenolic) and $NaOC_2H_5$ (carboxyl, lactonic, phenolic and carbonyls). The difference between the uptake of the bases can be used to identify and quantify the types of oxygen surface groups present on a carbon sample.

In this experiment, the sum of all oxygen surface groups was measured by this method as follows.

A mixture of about 1g hydrochar samples obtained from each run and 40.0 mL strong base, $NaOC_2H_5$ (0.0529 mol/L) was shaken for 2 h in 300 rpm and then put into a constant temperature environment of 25 ℃ for 24 h until all acidic surface functional groups on these samples had been totally neutralized by $NaOC_2H_5$. The mixtures were then filtered and the liquid parts were taken and diluted to 100 mL. HCl (0.0509 mol/L) was used to back-titrate the excess $NaOC_2H_5$ and the chemical gram equivalent of total acidic surface functional groups can be calculated by the equation as follow:

$$M = \left(\frac{c_{\mathrm{NaOC2H5}} V_{\mathrm{NaOC2H5}}}{1000} - \frac{c_{HCl} V_{HCl}}{1000}\right) / m_{HC} \qquad 3\text{-}8$$

(unit: eq/g)

Where: $c_{NaOC2H5}$ = the concentration of $NaOC_2H_5$ used to neutralize all acid functional groups (mol/L)

c_{HCl} = the concentration of HCl used in back titration (mol/L)

$V_{NaOC2H5}$ = the volume of $NaOC_2H_5$ used to neutralize all acid functional groups (mL)

V_{HCl} = the volume of HCl used in back titration (mL)

m_{HC} = the weight of hydrochar sample (g)

4. Synthesis and characteristics analysis of SCG hydrochar and SCG hydrochar derived activated carbon

This chapter is divided into two parts. In the first part, the synthesis of SCG hydrochar and its characteristics analysis at different hydrothermal treatment operating conditions will be discussed. In the second part, the synthesis of SCG hydrochar derived activated carbon and its characteristics analysis will be discussed. The mechanisms of hydrothermal carbonization of SCG and KOH chemical activation of SCG hydrochar will be discussed. Finally, a clarification of how hydrothermal treatment operating conditions affect the activated carbon will be made.

4.1 SCG hydrochar synthesis by hydrothermal carbonization

SCG hydrochar was successfully synthesized through hydrothermal treatment by the method described in section 3.2 of this thesis. In this section, the carbonization effect and surface characteristic properties of hydrochar synthesized under different HTC conditions was discussed. Finally, the speculated HTC reaction mechanism was proposed.

4.1.1 Carbonization effect on SCG samples by different SCG hydrochar synthesis operating conditions

4.1.1.1 Reaction temperature

To study the effect of temperature, the reaction temperature was changed from 180 ℃ to 300 ℃ at the reaction time of 2 h. The starting materials were dry SCG 4 g and deionized water 8g, and the reaction conditions are shown in Table 4-1, proximate analysis results which can reflect the carbonization degree are shown in Table 4-2 and Figure 4-1. High fixed carbon content and low volatile matter content represents high carbonization extent.

Table 4-1 Experimental conditions based on temperature variables

No.	Temperature	Reaction time	H_2O/SCG ratio	Presence of HNO_3
Run1	180℃	2h	2:1	0%
Run2	210℃			
Run3	240℃			
Run4	270℃			
Run5	300℃			

Table 4-2 Proximate value of Run1-5 after hydrothermal treatment

	Raw	Run1	Run2	Run3	Run4	Run5
VC%	86%	83%	78%	70%	67%	64%
FC%	13%	16%	21%	29%	32%	34%
Ash%	1%	1%	1%	1%	1%	2%
Yield%	/	85%	74%	62%	53%	48%
FC Yield%	/	14%	15%	18%	17%	16%

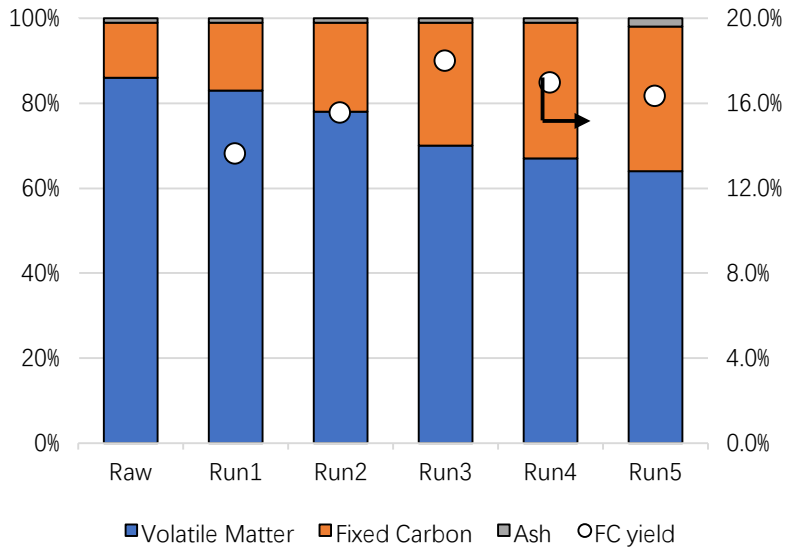

Figure 4-1 Summary of proximate value and fixed carbon yield of hydrochar obtained from Table 4-2

From Figure 4-1, we can tell that the proportion of fixed carbon content in the hydrochar product increased as reaction temperature increased. It indicates that the carbonization extent got further as the hydrothermal operating temperature arouse. From the date of FC yield%, we can see in relatively low

and high operating temperature, the fixed carbon conversion rate is lower than in the operating temperature of 240℃. It is probably because that in lower temperatures, lignin is too stable to decompose, and it can also interfere in the hydrolysis of cellulose and hemicellulose and slow the release of decomposition products formed from polysaccharides. [30] While in high temperatures, as the solid yield downtrend slows down, it can be speculated that more gaseous products rather than hydrochar generated from the material.

4.1.1.2 Reaction time

To study the effect of reaction time, the reaction time of 2 h and 4 h was picked with the reaction temperature of 180℃,240℃ and 300℃. The starting materials were dry SCG 4 g and deionized water 8g, and the reaction conditions are shown in Table 4-3, proximate analysis results which can reflect the carbonization degree are shown in Table 4-4 and Figure 4-2.

Table 4-3 Experimental conditions based on reaction time variables

No.	Temperature	Reaction time	H_2O/SCG ratio	Presence of HNO_3
Run1	180℃	2h	2:1	0%
Run2		4h		
Run3	240℃	2h		
Run4		4h		
Run5	300℃	2h		
Run6		4h		

Table 4-4 Proximate value of Run1-6 after hydrothermal treatment

	Run1	Run2	Run3	Run4	Run5	Run6
VC%	83%	74%	70%	67%	64%	63%
FC%	16%	24%	29%	31%	34%	34%
Ash%	1%	2%	1%	2%	2%	3%

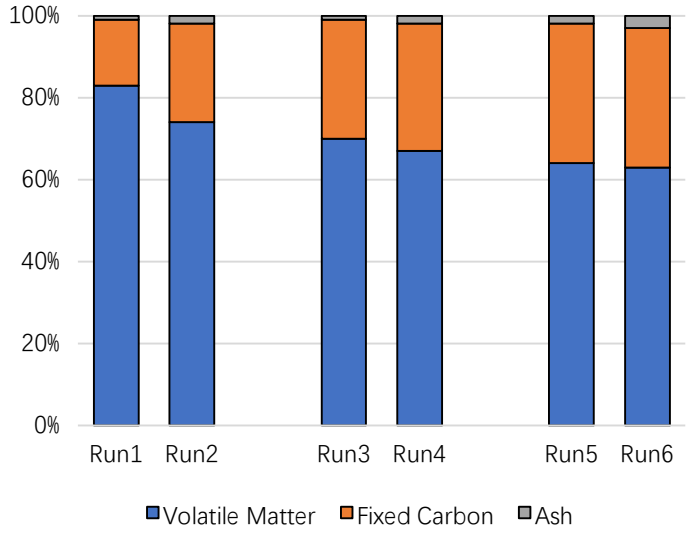

Figure 4-2 Summary of proximate value and solid yield of hydrochar obtained from Table 4-4

From Figure 4-2, we can tell that longer HTC reaction time cause further carbonization on the samples treated in the same conditions. Especially in low temperature, fixed carbon content increased obviously. It might be due to the combined effect of the increase in polymerization and the formation of secondary hydrochar along with the decomposition of biomass to liquid/gaseous products. [41]

4.1.1.3 H_2O/SCG ratio

To study the effect of H_2O/SCG ratio, the H_2O/SCG ratio of 2:1 and 5:1 was picked with the reaction temperature of 180 ℃, 240 ℃ and 300 ℃. The reaction conditions are shown in Table 4-5, proximate analysis results which can reflect the carbonization degree are shown in Table 4-6 and Figure 4-3.

Table 4-5 Experimental conditions based on water volume variables

No.	Temperature	Reaction time	H_2O/SCG ratio	Presence of HNO_3
Run1	180℃	2h	2:1	0%
Run2			5:1	
Run3	240℃		2:1	
Run4			5:1	
Run5	300℃		2:1	
Run6			5:1	

Table 4-6 Proximate value of Run1-6 after hydrothermal treatment

	Run1	Run2	Run3	Run4	Run5	Run6
VC%	83%	78%	70%	68%	64%	60%
FC%	16%	21%	29%	31%	34%	38%
Ash%	1%	1%	1%	1%	2%	2%

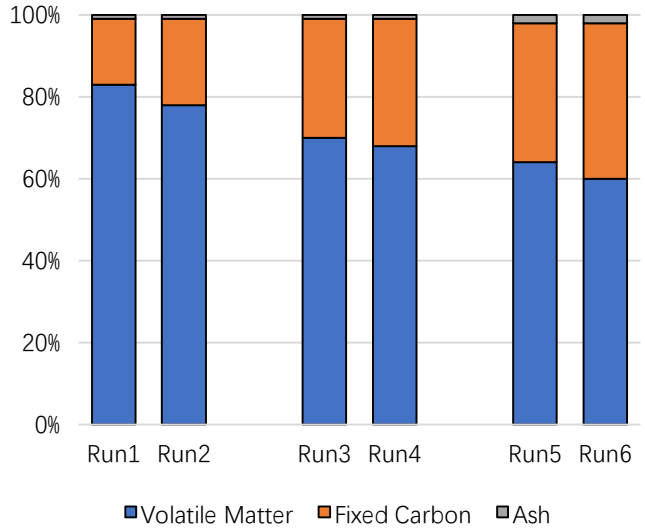

Figure 4-3 Summary of proximate value and solid yield of hydrochar obtained from Table 4-6

From Figure 4-3, we can see that high weight ratio of H_2O/SCG cause further carbonization on the samples treated in the same conditions. Because in the case of high weight ratio of H_2O/SCG, extensive hydrolysis took place at SCG substrate (water is more), most of the dissolved products might have undergone condensation and thus improved the carbonization extent.

4.1.1.4 HNO_3 additive

To study the effect of HNO_3 assist in hydrothermal treatment, experiments in the same HTC operating conditions as shown in Table 4-1 were conducted with 5% HNO_3 acid addition. The reaction conditions are shown in Table 4-7, proximate analysis results which can reflect the carbonization degree are shown in Table 4-8 and Figure 4-4.

Table 4-7 Experimental conditions based on HNO_3 additive variables

No.	Temperature	Reaction time	H_2O/SCG ratio	Presence of HNO_3
Run1	180℃	2h	2:1	0%
Run2	210℃			
Run3	240℃			
Run4	270℃			
Run5	300℃			
Run6	180℃			5%
Run7	210℃			
Run8	240℃			
Run9	270℃			
Run10	300℃			

Table 4-8 Proximate value of Run1-5 after hydrothermal treatment

	Run1	Run2	Run3	Run4	Run5
VC%	83%	78%	70%	67%	64%
FC%	16%	21%	29%	32%	34%
Ash%	1%	1%	1%	1%	1%
Yield%	85%	74%	62%	53%	48%
FC Yield%	14%	22%	15%	20%	18%
	Run6	Run7	Run8	Run9	Run10
VC%	69%	68%	60%	58%	53%
FC%	29%	30%	37%	39%	44%
Ash%	1%	1%	2%	1%	2%
Yield%	77%	68%	60%	51%	36%
FC Yield%	22%	17%	20%	16%	17%

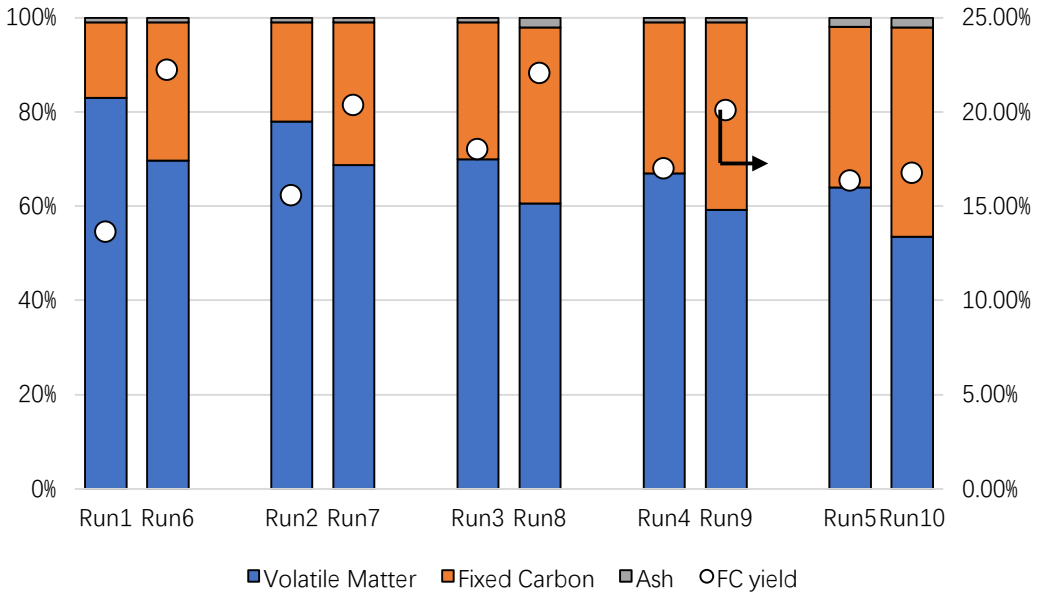

Figure 4-4 Summary of proximate value and fixed carbon yield of hydrochar obtained from Table 4-8

From Figure 4-4, we can see 5% HNO_3 assisted HTC contributed more to carbonization extent. This is because that HNO_3 in the solution promotes the hydrolysis of cellulosic fraction and polymerization of monomer decomposed from cellulosic fraction. The FC yield% of 5% HNO_3 assisted HTC also reflect the same result.

4.1.2 Characteristics analysis of SCG hydrochar

Several of hydrochar products synthesized from Table 4-7 were subject to characteristics analysis, which can help a lot to understand the formation process of hydrochar. Note that these hydrochars are named as (m)x-HC, where m represents HNO_3 modification, x represents HTC temperature, HC represents hydrochar.

4.1.2.1 Surface functional groups analysis

Chemical gram equivalent of hydrochar's total acidic surface functional groups was determined by Boehm titration. Results are shown in Table 4-9 and Figure 4-5.

Table 4-9 Total acidic surface functional groups of hydrochar obtained from all runs

	Raw	180-HC	210-HC	240-HC	270-HC	300-HC
Total acidic surface functional groups (meq/g)	1.01	1.10	1.13	1.06	1.04	0.933

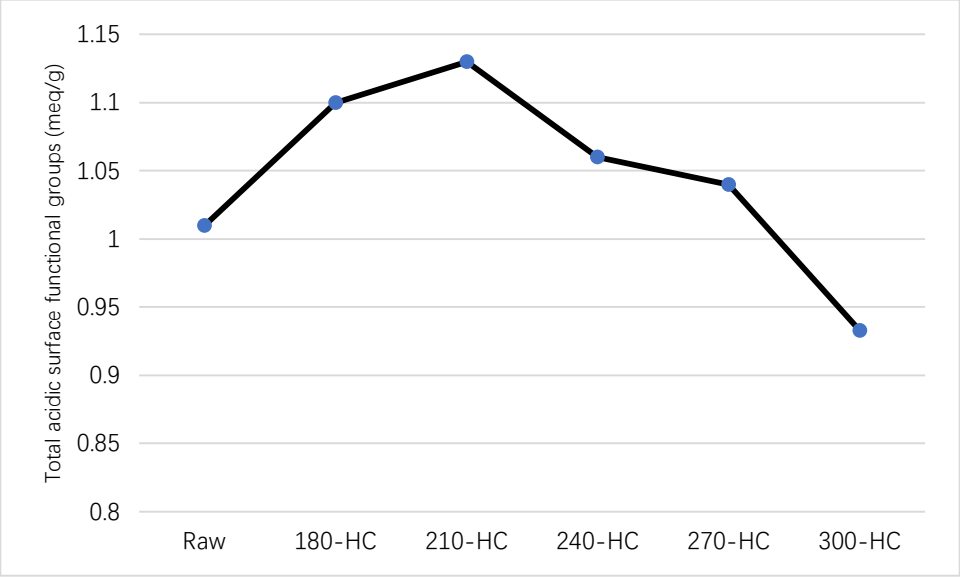

Figure 4-5 Total acidic surface functional groups of hydrochars obtained from all runs

From Figure 4-5, we can see that total acid functional groups amount is high in 210 ℃ while relatively lower in relatively low temperature and high temperature. Probably it is because in relatively lower reaction temperature, the cellulosic matter is too stable to be decomposed into soluble monomers to form acidic functional groups. While in relatively high reaction temperature, the decomposition speed of acidic functional groups is higher than the formation speed of acidic functional groups.

4.1.2.2 Morphology analysis

The surface morphology of SCG raw material, SCG hydrochar synthesized by HTC under 240℃ and SCG hydrochar synthesized by HNO_3 assisted HTC under 240℃ were observed by SEM as shown in Figure 4-6, 4-7, 4-8.

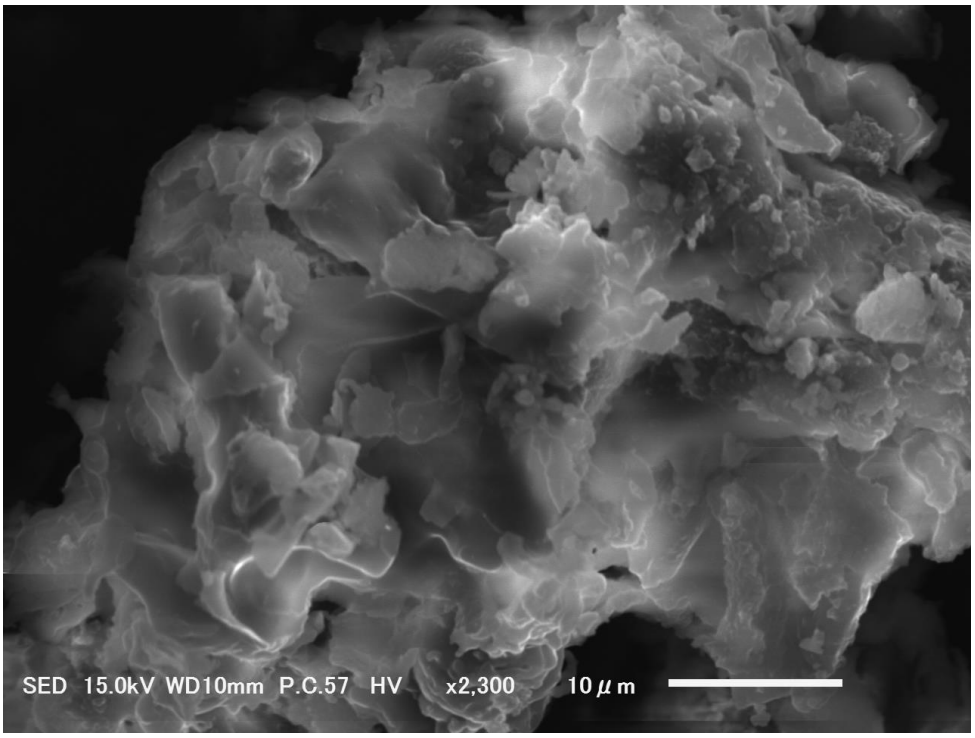

Figure 4-6 SEM image of SCG raw material

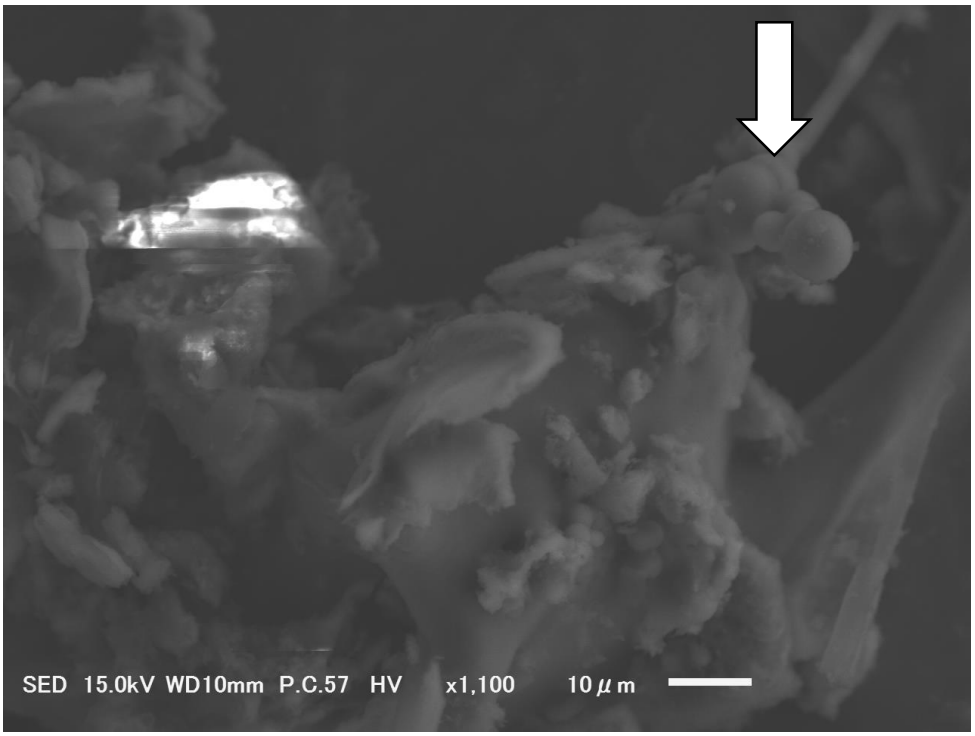

Figure 4-7 SEM image of SCG hydrochar synthesized by HTC under 240℃

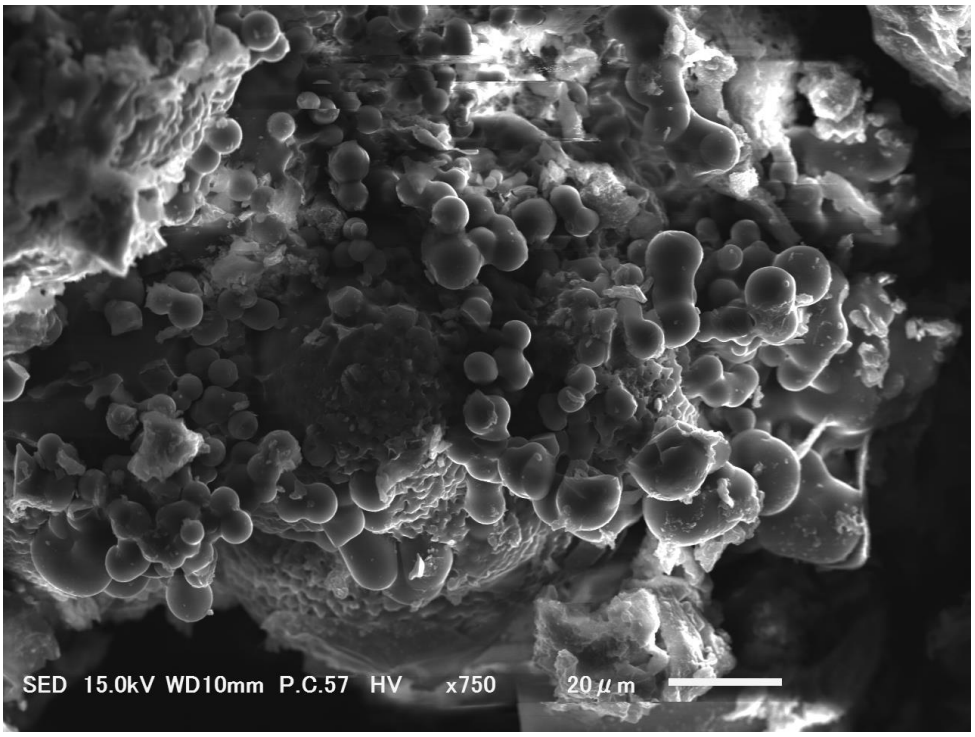

Figure 4-8 SEM image of SCG hydrochar synthesized by HNO_3 assisted HTC under 240℃

The image of Figure 4-7 revealed that the particles retain the appearance of the raw material as shown in Figure 4-6. The spheres observed as marked by the arrow, are assumed as the carbon microspheres derived from cellulosic fraction. Addition of HNO_3 promoted the hydrolysis of the organic substrate and facilitated the dehydration of decomposed soluble matter to form carbon microspheres in HTC process as shown in Figure 4-8. These results explain why fixed carbon content is higher with hydrochar prepared under HNO_3 assisted HTC.

4.1.3 Speculated HTC reaction mechanism of SCG

As SCG comprises different polymer chains, the mechanism for conversion from SCG raw material to SCG hydrochar is quite complex. Cellulose, hemicellulose and lignin consisted in SCG are considered to be the main constituents that contribute to form SCG hydrochar.

A simple route of speculated HTC conversion from SCG raw material to SCG hydrochar is shown in Figure 4-9.

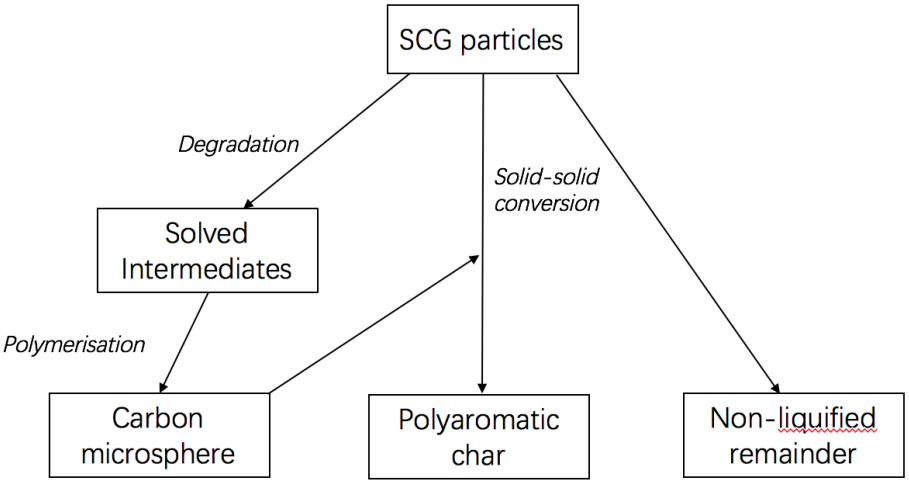

Figure 4-9 Speculated HTC mechanism process from SCG to hydrochar

There are two main routes of hydrochar formation. One route is direct solid-solid conversion. Biomass matter like non-dissloved lignin which is not exposed to the water undergoes pyrolysis process to form polyaromatic char, and other biomass matter which does not participate in hydrolysis converts into other non-liquidized biomass derivative. Another route is liquid-solid conversion. Biomass matter like cellulose are hydrolyzed into different small solved oligomers, and then these oligomers undergo complex reactions to produce polymers and carbon microsphere with high OFGs in their surface like shown in Figure 4-8.

4.2 Activated carbon synthesis from SCG hydrochar by KOH chemical activation

Besides the utilization of adsorbent, SCG hydrochar can also be prepared as a good precursor for the synthesis of porous activated carbon via KOH chemical activation because of its high surface functionalization and low condensation degree. These characteristics make the hydrochar precursor highly reactive and the reactivity of the precursor is a key parameter in the chemical activation process. [42] In this section, activation effect on hydrochar and the relationship between the activated carbon's physicochemical properties and its corresponding hydrochar precursor's HTC conditions were discussed.

4.2.1 Activation of SCG hydrochar

Hydrochar synthesized through hydrothermal treatment in 240 ℃ (240-HC) and activated carbon synthesized from the former hydrochar through KOH chemical activation (240-AC) were characterized by N_2 gas sorption test. The N_2 gas sorption isotherm and corresponding analysis results are shown in Figure 4-10, Figure 4-11 and Table 4-10.

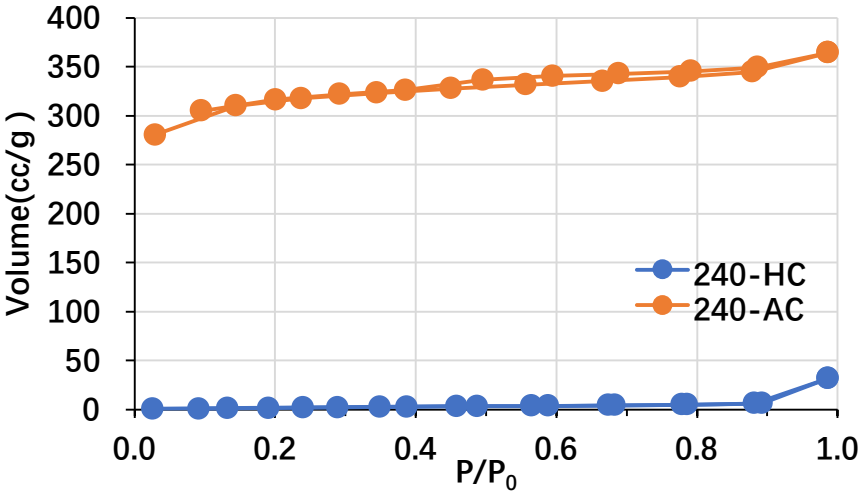

Figure 4-10 N_2 sorption isotherm of samples before and after KOH activation

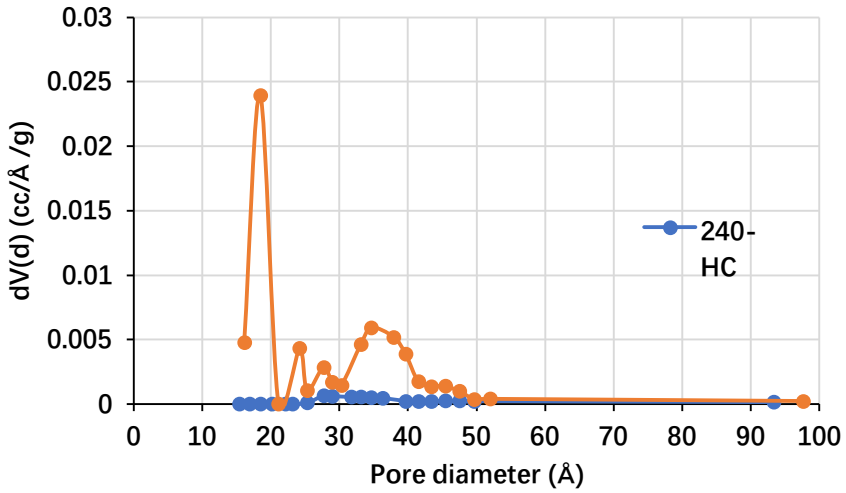

Figure 4-11 Pore size distribution of samples before and after KOH activation

Table 4-10 Pore volume and surface area of samples before and after KOH activation

Sample name	Pore volume (cc/g)	BET surface area (m^2/g)
240-HC	0.009	3.887
240-AC	0.485	916.0

As we can see from Figure 4-10, Figure 4-11 and Table 4-10, it is evident that for the SCG precursor, the KOH chemical activation leads to a complete change in pore size distribution, pore volume and surface area.

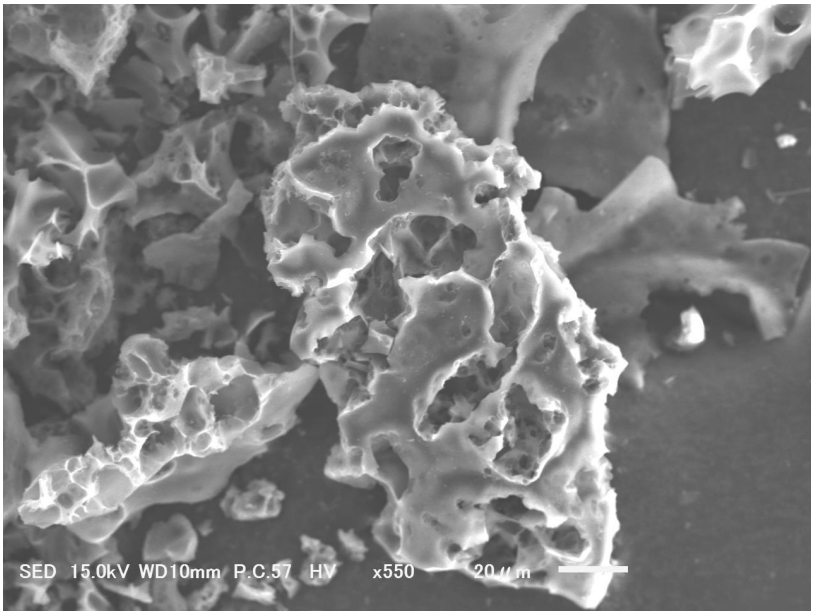

Figure 4-12 SEM image of activated carbon synthesized from 240-HC

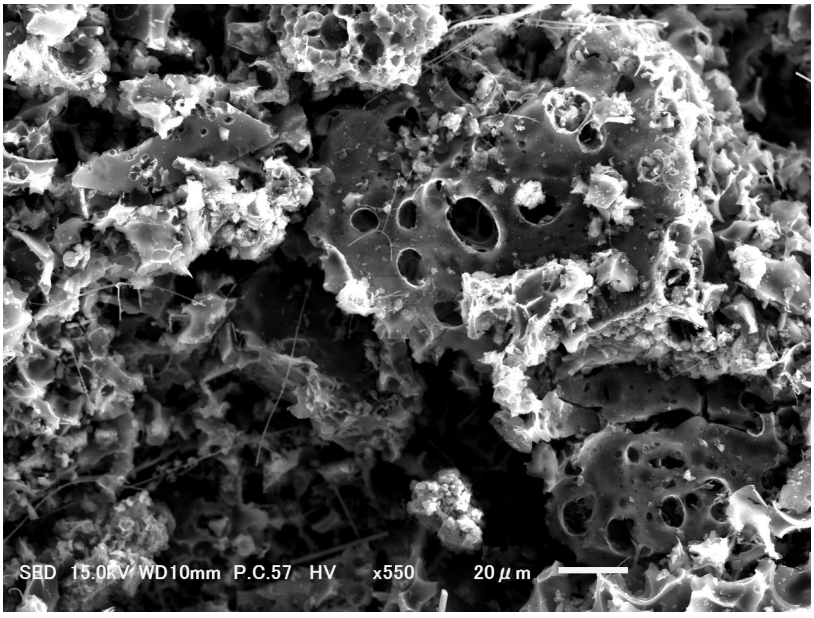

Figure 4-13 SEM image of activated carbon synthesized from m240-HC

Figure 4-12 and Figure 4-13 are SEM images of activated carbon synthesized from hydrochar prepared under 240 ℃ HTC treatment and 240 ℃ 5% HNO_3 assisted HTC treatment, which also indicate that a drastic morphological transformation took place during the chemical activation process.

4.2.2 Activation effect of activated carbon derived from hydrochar prepared under different HTC pretreatment operating conditions

In this section, the relationship between the HTC pretreatment operating conditions in SCG hydrochar precursor preparation and the activation extent of the SCG hydrochar derived activated carbons was investigated.

For the purpose of this investigation, some activated carbon samples derived from SCG hydrochar were picked as shown in Table 4-11, samples are named as (m)x-AC, where x represents the HTC temperature of the hydrochar precursor, m represents HNO_3 acid modification, AC represents activated carbon.

Table 4-11 Activated carbon precursor's HTC synthesis conditions

Sample name	Temperature (℃)	Time (min.)	HNO_3 Conc. (%)
180-AC	180	120	0
240-AC	240	120	0
300-AC	300	120	0
m180-AC	180	120	5
m240-AC	240	120	5
m300-AC	300	120	5

4.2.2.1 Temperature

The HTC operating temperature is influential in affecting the porosity development and pore size distribution of the activated carbon synthesized from hydrochar. The relationship between the HTC pretreatment operating temperatures in precursor synthesis and the activation extent of the activated carbons derived from these precursors as well as the practical adsorption performance test were investigated. Activated carbons derived from hydrochars prepared through HTC treatment under 180℃, 240℃, 300℃ were chosen for test and further analyzation.

Figure 4-14 reveals that 240-AC has the largest N_2 uptake, arising from a higher porosity development than in the cases of 180-AC, 300-AC. From Figure 4-15, we can see that 240-AC presents larger contribution of broader pores than other activated carbons. It can also be told from Table 4-12 that 240-AC has the largest pore volume and surface area.

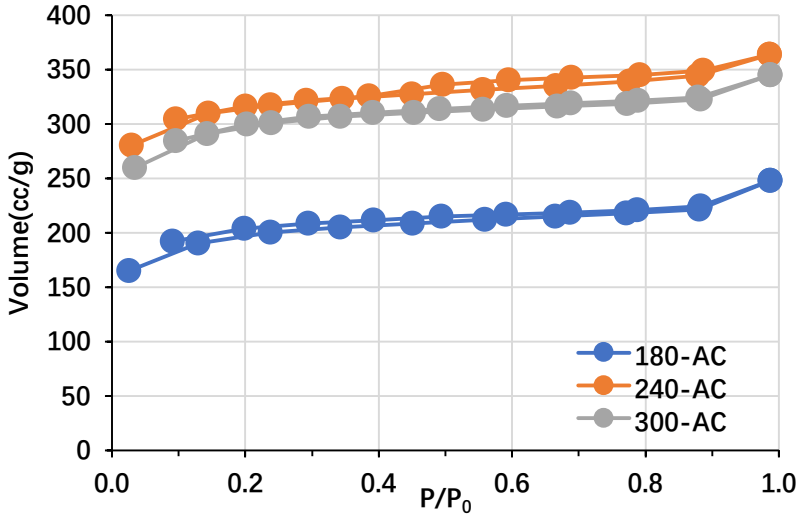

Figure 4-14 N_2 sorption isotherm of activated carbons (hydrochar samples after KOH activation)

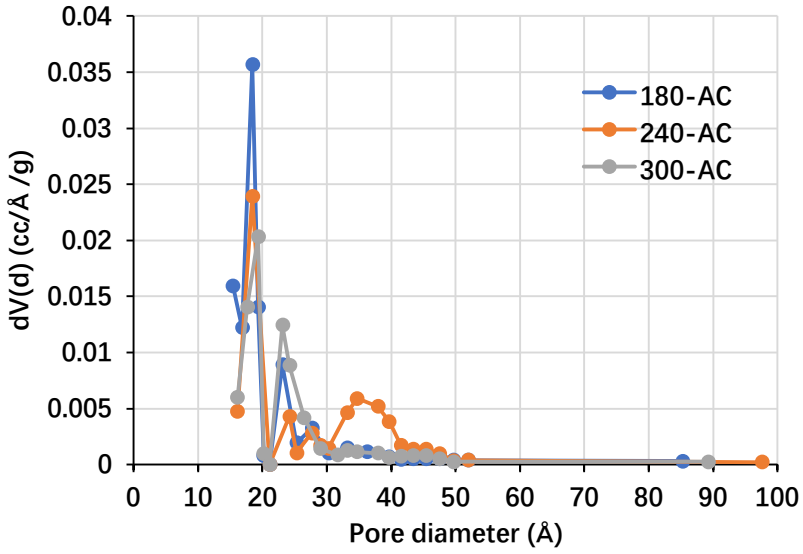

Figure 4-15 Pore size distribution of activated carbons (hydrochar samples after KOH activation)

Table 4-12 Pore volume and surface area of activated carbons (hydrochar samples after KOH activation)

Sample name	Pore volume (cc/g)	BET surface area (m^2/g)
180-AC	0.311	542.4
240-AC	0.485	916.0
300-AC	0.451	793.2

The reason why 240-AC has the most developed porosity could be explained by that during KOH activation, H^+ ion in carboxyl groups and hydroxyl groups is easily exchanged by K^+, which affects the electron cloud distribution of aromatic carbon, increases the active point of carbon material and makes the material easier to be activated. Thus, it could be speculated that in the surface of 240-AC's precursor, the amount of carboxyl groups and hydroxyl groups are higher than the other two activated carbon's precursors.

4.2.2.2 HNO_3 acid modification

The effect of activated carbon synthesized from hydrochar prepared by HNO_3 assisted HTC were investigated. Figure 4-16, Figure 4-17 and Table 4-

13 shows that 5% HNO_3 assisted HTC of hydrochar did not improve the pore development of the corresponding activated carbon.

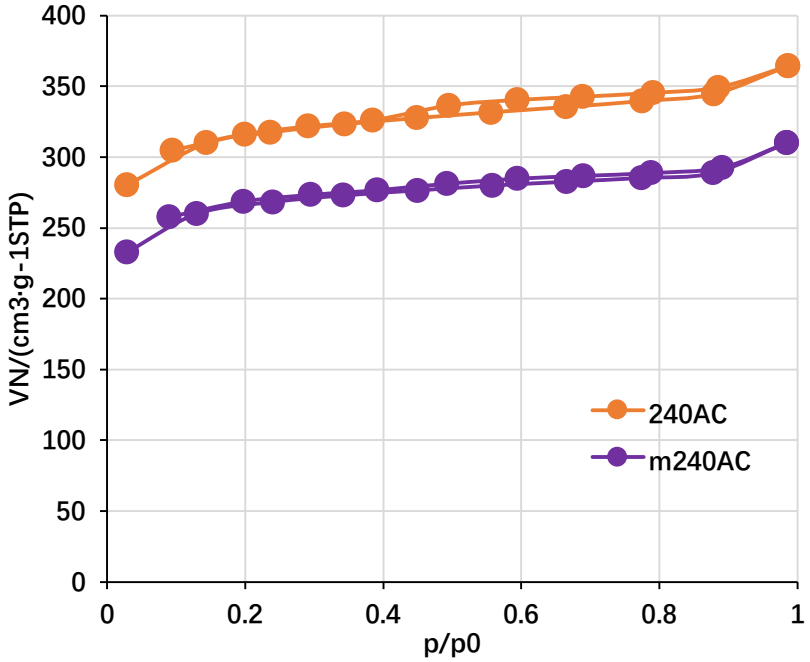

Figure 4-16 N_2 sorption isotherm of activated carbons (hydrochar precursor synthesized by HTC and HNO_3 assisted HTC)

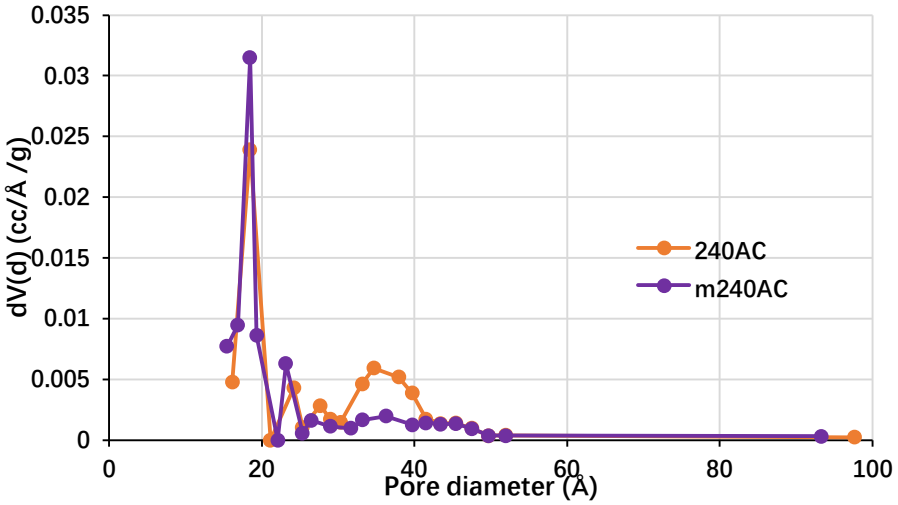

Figure 4-17 Pore size distribution of activated carbons (hydrochar precursor synthesized by HTC and HNO_3 assisted HTC)

Table 4-13 Pore volume and surface area of activated carbons (hydrochar precursor synthesized by HTC and HNO_3 assisted HTC)

Sample name	Pore volume (cc/g)	BET surface area (m^2/g)
240-AC	0.485	916.0
m240-AC	0.405	765.3

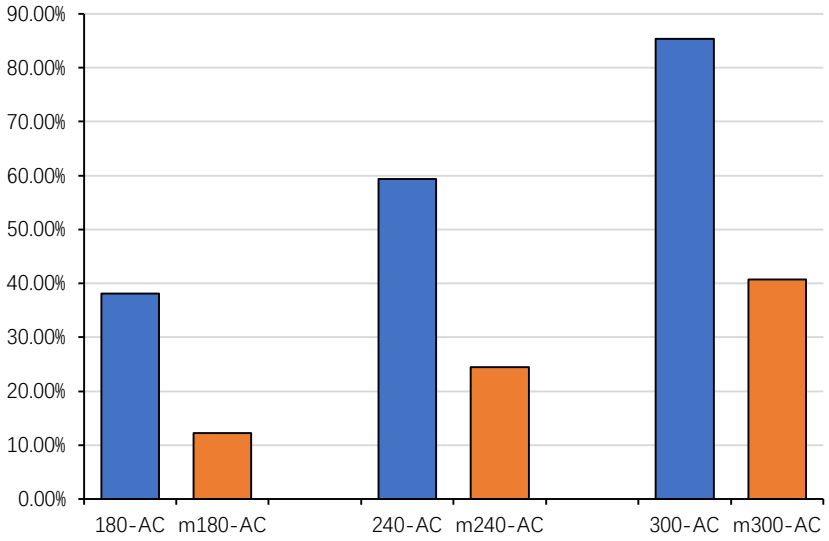

Figure 4-18 Mass yield of activated carbons of Table 4-13

The mass yield of these products after KOH activation are shown in Figure 4-18. We can tell that the mass yield of hydrochars prepared from 5% HNO_3 assisted HTC was obviously lower than those prepared from traditional HTC process while the fixed carbon content of these hydrochar is higher. This may give a good explanation of the reason why HNO_3 assisted HTC did not improve the pore development of the corresponding activated carbon. The low mass yield indicates that activation is too intense to destroy a lot of pores and more gaseous products are produced from the destruction. The intensity of KOH activation is mainly due to the high chemical reactivity of hydrochar like high OFGs content. Maybe KOH activation conditions should be adjusted to obtain high quality activated carbon.

5. Application of SCG hydrochar and derived activated carbon as adsorbent in water treatment

5.1 Application of SCG hydrochar in water treatment

A model heavy metal, zinc, and a model organic dye, Rhodamine B, were used in adsorption performance experiment. Adsorbents were picked from hydrochar synthesized in different HTC operating conditions. The relationship between their adsorption amount and their preparation conditions of HTC was investigated.

5.1.1 Effect of hydrochar's HTC temperature on its zinc and Rhodamine B adsorption performance

The zinc and Rhodamine B adsorption performance experiments of hydrochar prepared by HTC under different temperatures shown in Table 5-1 was conducted. Zinc adsorption performance result is shown in Figure 5-1, and RhB adsorption performance result is shown in Figure 5-2.

Table 5-1 Experimental conditions based on temperature variables

No.	Temperature	Reaction time	H_2O/SCG ratio	Presence of HNO_3
Run1	180℃	2h	2:1	0%
Run2	210℃			
Run3	240℃			
Run4	270℃			
Run5	300℃			

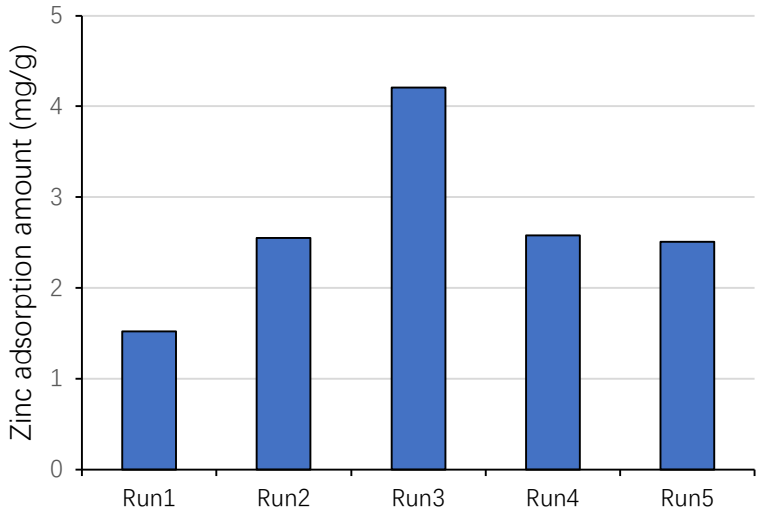

Figure 5-1 Zinc adsorption amount by hydrochar from all runs shown in Table 5-1

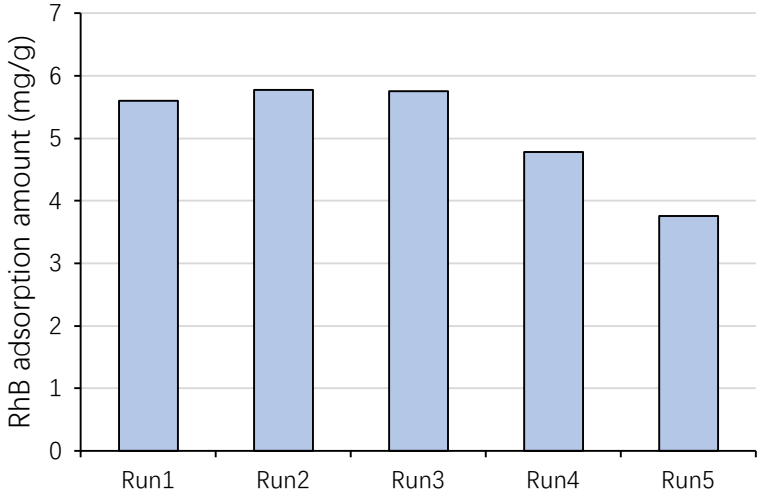

Figure 5-2 Rhodamine B adsorption amount by hydrochar from all runs shown in Table 5-1

From Figure 5-1 and Figure 5-2, we can see that Run 3 (hydrochar synthesized under 240℃) shows the highest adsorption amount of both model contaminants. Probably this is because chemical adsorption is the main

mechanism in the case of SCG hydrochar and 240-HC from Run 3 owned more OFGs. It was considered that more OFGs, especially the carboxyl groups and hydroxyl groups, could offer more exchangeable H^+ ion to adsorb zinc ion by electrostatic interaction. Thus, at a lower HTC temperature, cellulosic matters were too stable to be decomposed, so the content of OFGs content was low. In contrast, the condensation of hydrochar and decomposition of OFGs are likely to take place excessively at higher HTC temperature.

5.1.2 Effect of hydrochar's HTC reaction time on its zinc and Rhodamine B adsorption performance

The zinc and Rhodamine B adsorption performance experiments of hydrochar prepared by HTC under different reaction time shown in Table 5-2 was conducted. Zinc adsorption performance result is shown in Figure 5-3, and RhB adsorption performance result is shown in Figure 5-4.

Table 5-2 Experimental conditions based on reaction time variables

No.	Temperature	Reaction time	H_2O/SCG ratio	Presence of HNO_3
Run1	180℃	2h	2:1	0%
Run2		4h		
Run3	240℃	2h		
Run4		4h		
Run5	300℃	2h		
Run6		4h		

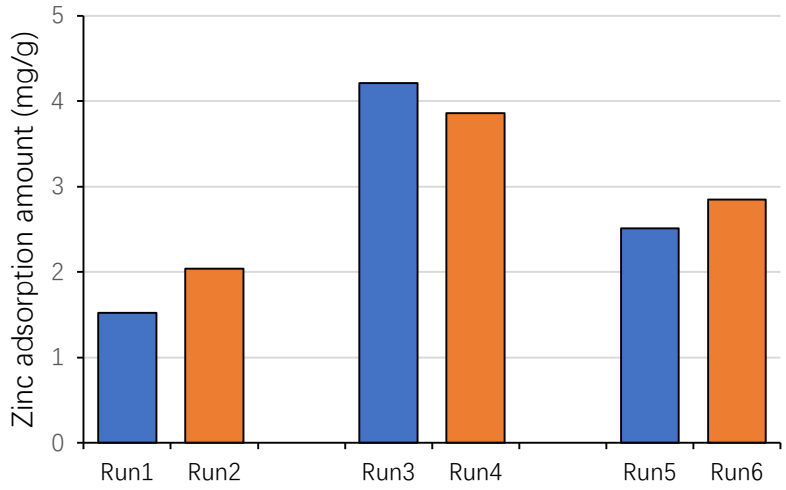

Figure 5-3 Zinc adsorption amount by hydrochar from all runs shown in Table 5-2

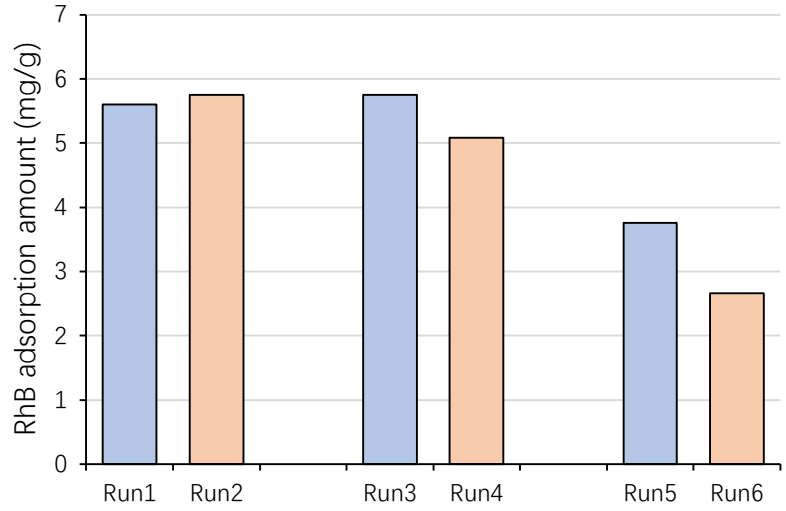

Figure 5-4 Rhodamine B adsorption amount by hydrochar from all runs shown in Table 5-2

From Figure 5-3 and Figure 5-4, the effect of HTC reaction temperature with reaction time of 2 h and 4 h shows the same trend of adsorption performance of both model contaminants.

5.1.3 Effect of hydrochar's HTC reaction SCG/water ratio on its zinc and Rhodamine B adsorption performance

The zinc and Rhodamine B adsorption performance experiments of hydrochar prepared by HTC under different SCG/water ratio shown in Table 5-3 was conducted. Zinc adsorption performance result is shown in Figure 5-5, and RhB adsorption performance result is shown in Figure 5-6.

Table 5-3 Experimental conditions based on water volume variables

No.	Temperature	Reaction time	H_2O/SCG ratio	Presence of HNO_3
Run1	180℃	2h	2:1	0%
Run2			5:1	
Run3	240℃		2:1	
Run4			5:1	
Run5	300℃		2:1	
Run6			5:1	

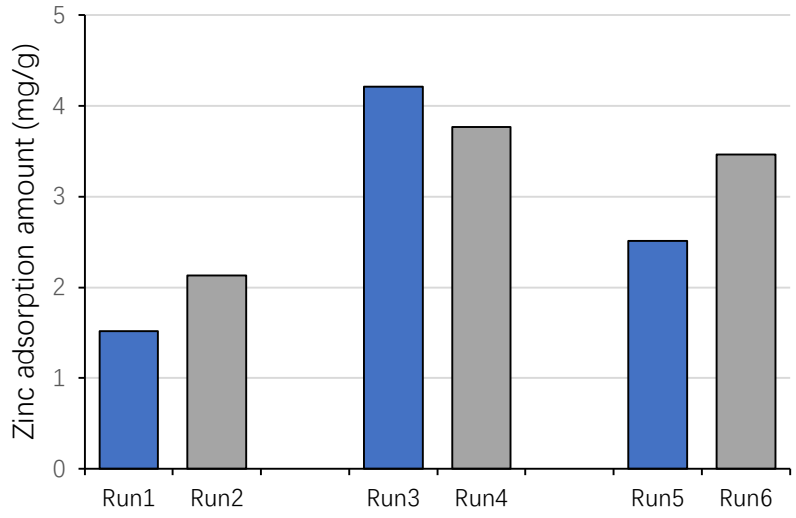

Figure 5-5 Zinc adsorption amount by hydrochar from all runs shown in Table 5-3

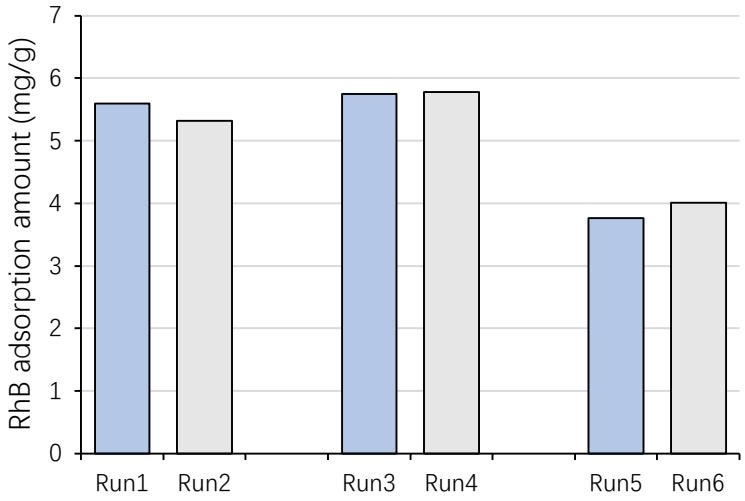

Figure 5-6 Rhodamine B adsorption amount by hydrochar from all runs shown in Table 5-3

From Figure 5-5 and Figure 5-6, the effect of HTC reaction temperature with SCG/water ratio of 1:2 and 1:5 shows the same trend of adsorption performance of both model contaminants.

5.2 Application of SCG hydrochar derived activated carbon in water treatment

A model heavy metal, zinc, was used in adsorption performance experiment. Adsorbents were picked from activated carbon synthesized from hydrochar prepared in different HTC operating conditions. The relationship between their adsorption capacity and their preparation conditions of HTC was investigated.

5.2.1 Effect of hydrochar prepared from different HTC temperature on its corresponding activated carbon's zinc adsorption performance

A comparative study involving the isotherms corresponding to the zinc adsorption performance experiments by activated carbons derived from

hydrochar prepared through HTC treatment under 180℃, 240℃, 300℃ is illustrated in Figure 5-7, 5-8, 5-9.

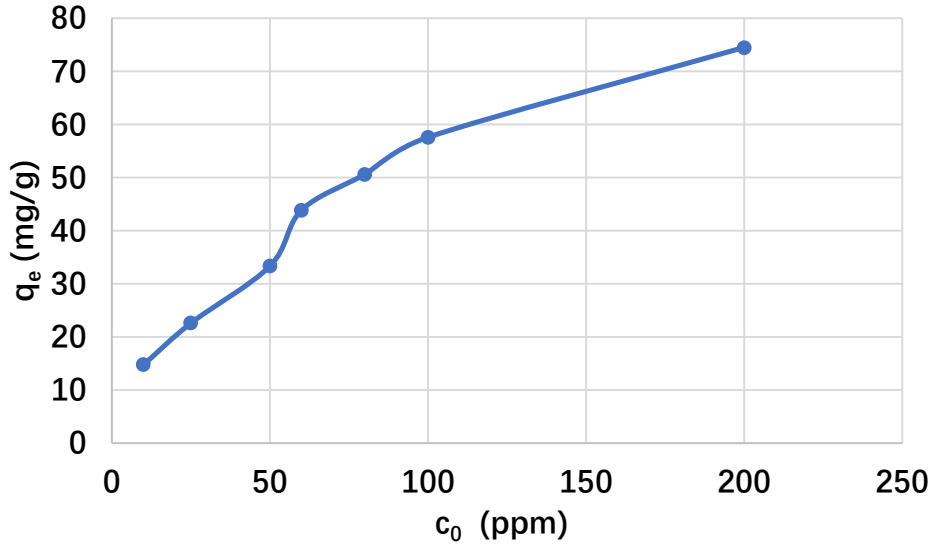

Figure 5-7 Adsorption isotherm of zinc for 180-AC

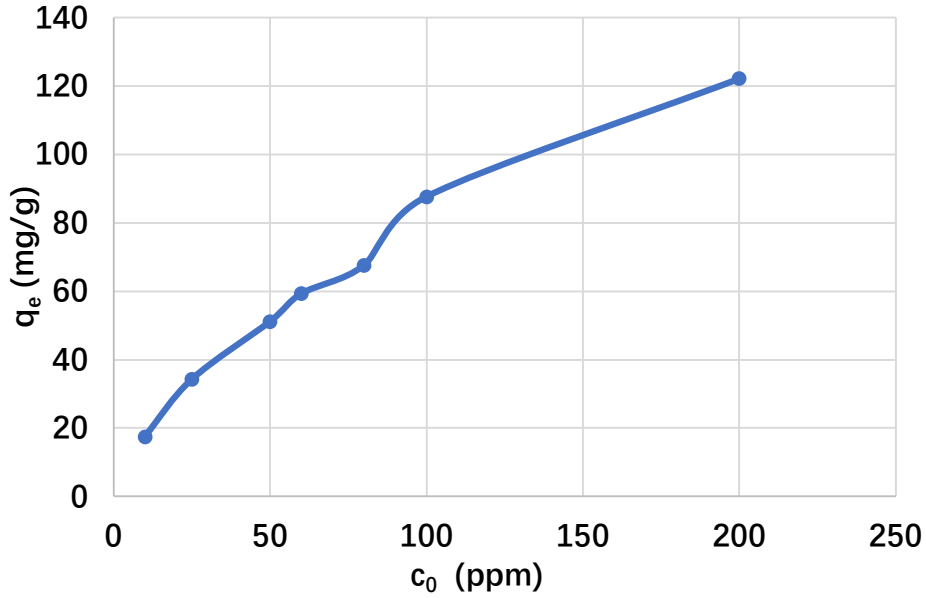

Figure 5-8 Adsorption isotherm of zinc for 240-AC

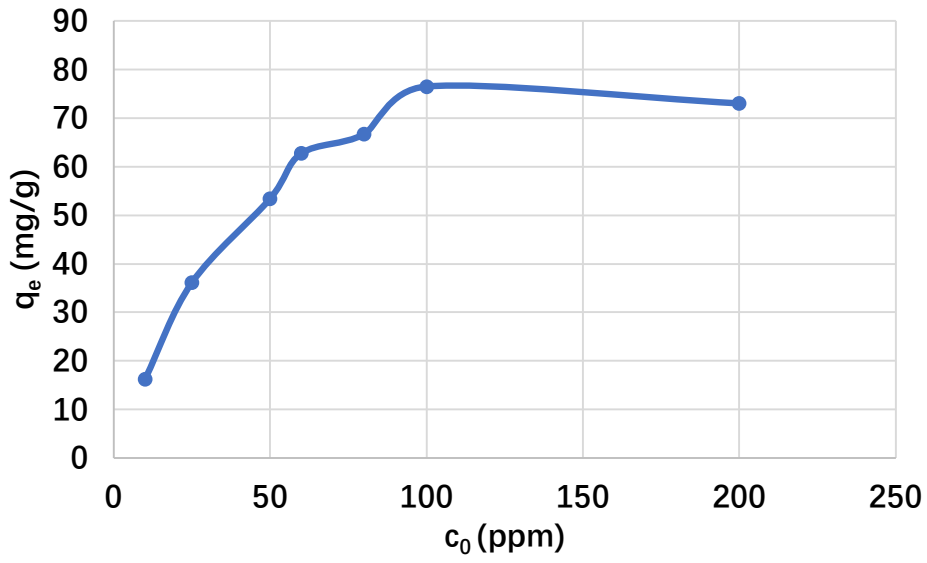

Figure 5-9 Adsorption isotherm of zinc for 300-AC

Langmuir equation is based on a theoretical model and assumes that the maximum adsorption corresponds to a monolayer saturated with adsorbate molecules on the adsorbent surface that is energetically homogeneous.

$q_e = K_L q_m C_e / (1 + K_L C_e)$ is the original equation form of Langmuir equation, and it can be changed into $C_e/q_e=1/K_L q_m+C_e/q_m$, where K_L is a parameter which make reference to the adsorption energy and q_m is a constant relative to the maximum adsorption capacity. Then results obtained for each AC adsorbent were fit to the changed Langmuir equation as illustrated in Figure 5-10, 5-11, 5-12, respectively.

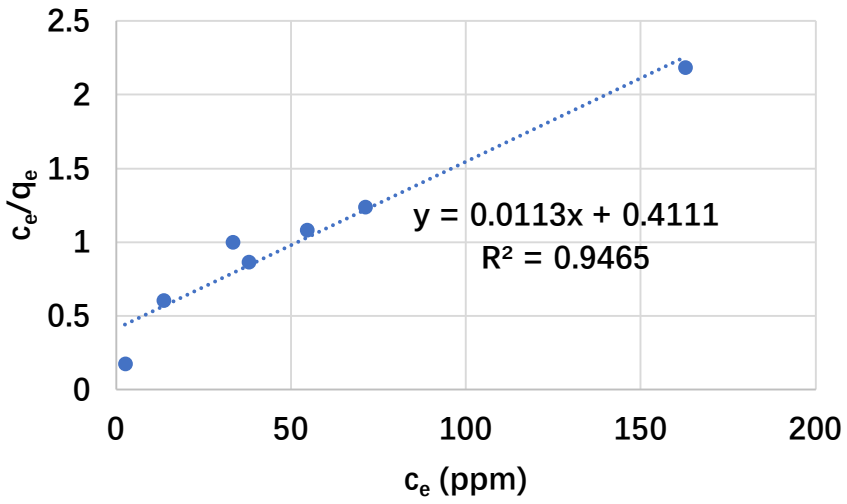

Figure 5-10 Langmuir's isotherm of zinc adsorption by 180AC

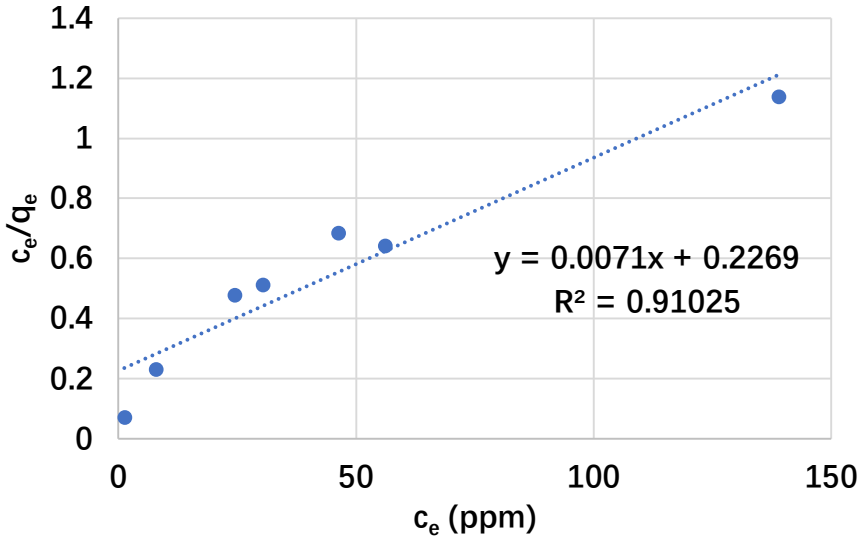

Figure 5-11 Langmuir's isotherm of zinc adsorption by 240AC

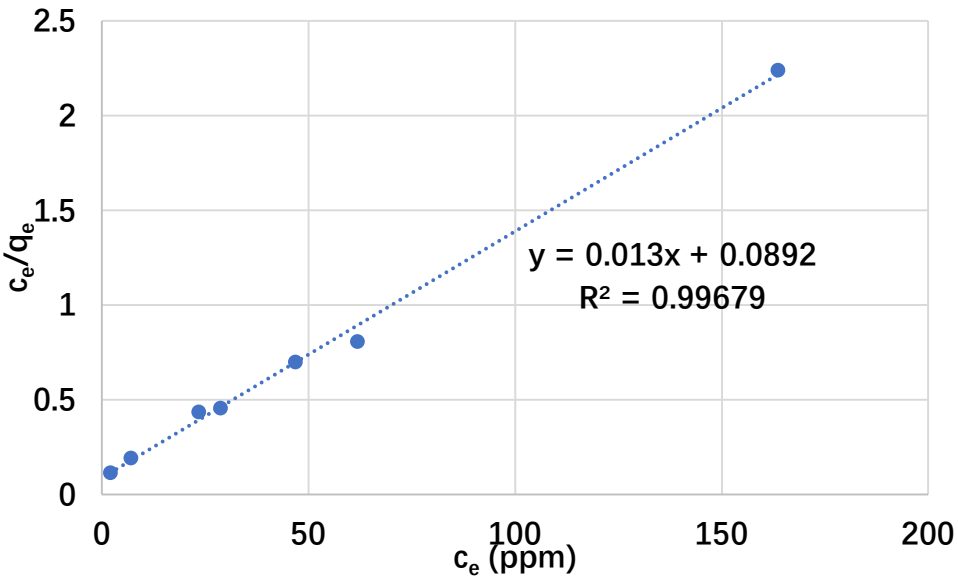

Figure 5-12 Langmuir's isotherm of zinc adsorption by 300AC

The zinc adsorption capacity results from fitting to Langmuir models are shown in Table 5-4. Activated carbon under HTC pretreatment operating temperature at 240℃ (240-AC) showed the highest zinc ion adsorption capacity among all samples with other same synthesis conditions.

Table 5-4. Zinc ion adsorption capacity of activated carbons (hydrochar samples after KOH activation)

Sample name	Adsorption capacity (mg/g)
180-AC	88.5
240-AC	140.9
300-AC	76.9

5.2.2 Effect of hydrochar prepared from 5% HNO_3 assisted HTC on its corresponding activated carbon's zinc adsorption performance

To compare the zinc adsorption performance of activated carbon which are derived from hydrochar prepared by 5% HNO_3 assisted HTC to the one from normal HTC, isotherms corresponding to the zinc adsorption performance

experiments by activated carbons derived from hydrochar prepared through 5% HNO_3 assisted HTC treatment under 180℃, 240℃, 300℃ is illustrated in Figure 5-13, 5-14, 5-15.

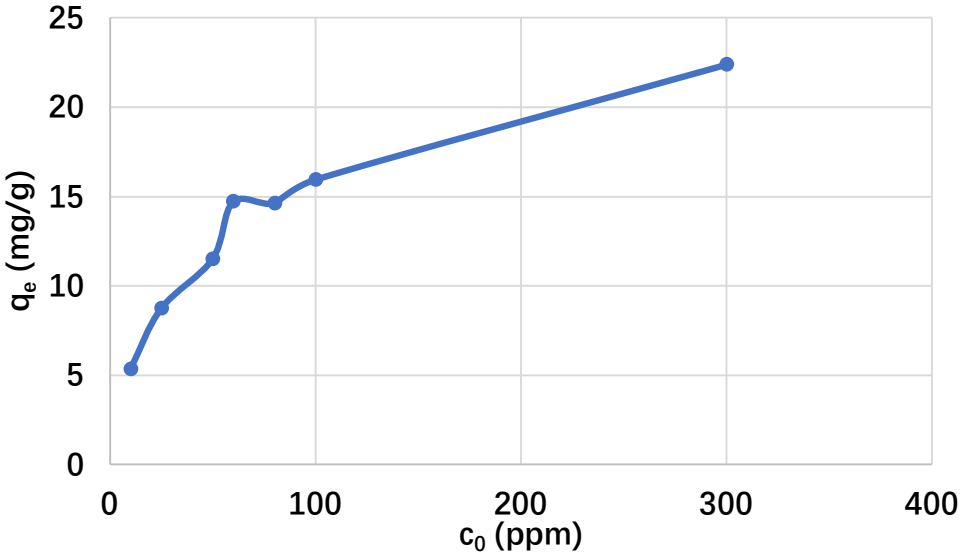

Figure 5-13 Adsorption isotherm of zinc for m180-AC. mAC=0.05g; T=25℃.

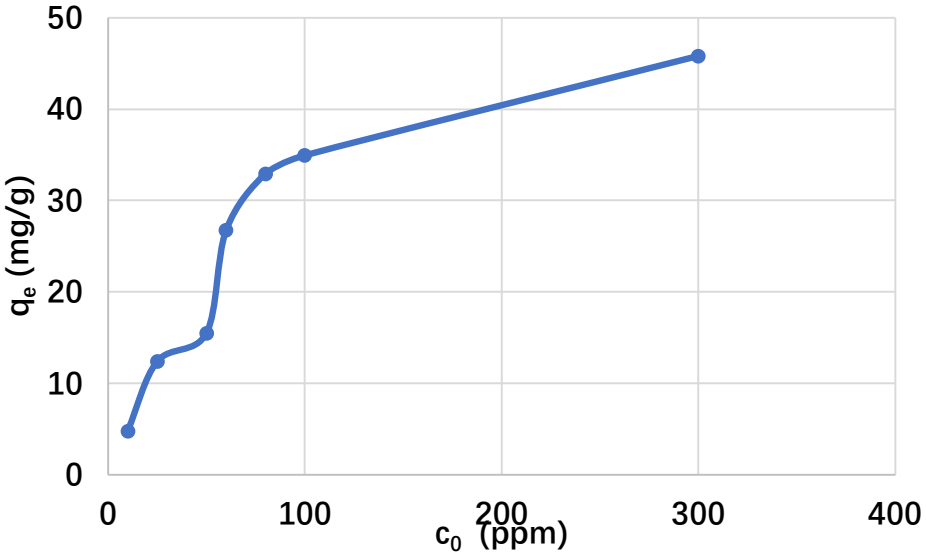

Figure 5-14 Adsorption isotherm of zinc for m240-AC. mAC=0.05g; T=25℃.

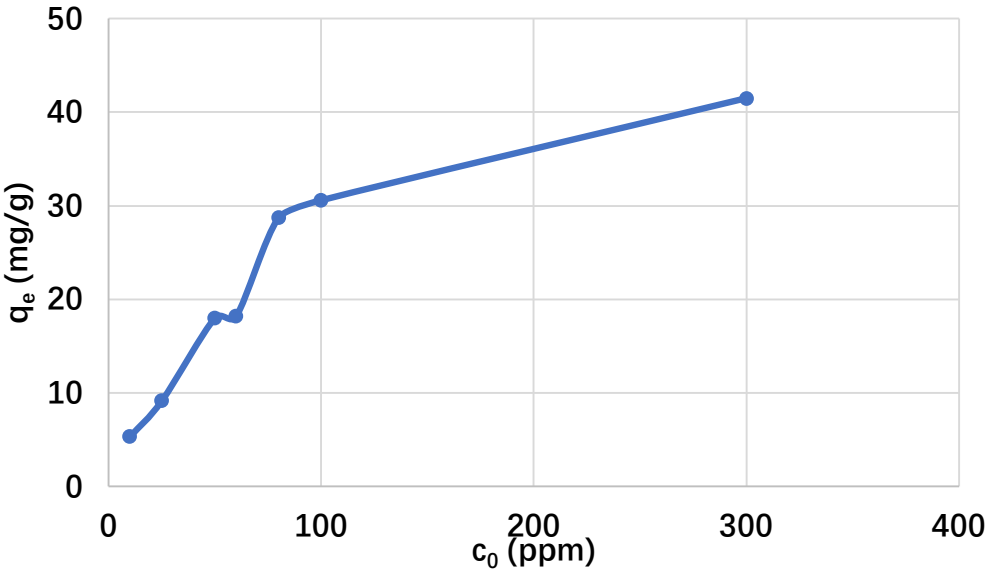

Figure 5-15 Adsorption isotherm of zinc for m300-AC. mAC=0.05g; T=25℃.

Then, results obtained for each AC adsorbent were fit to the Langmuir equation as illustrated in Figure 5-16, 5-17, 5-18, respectively.

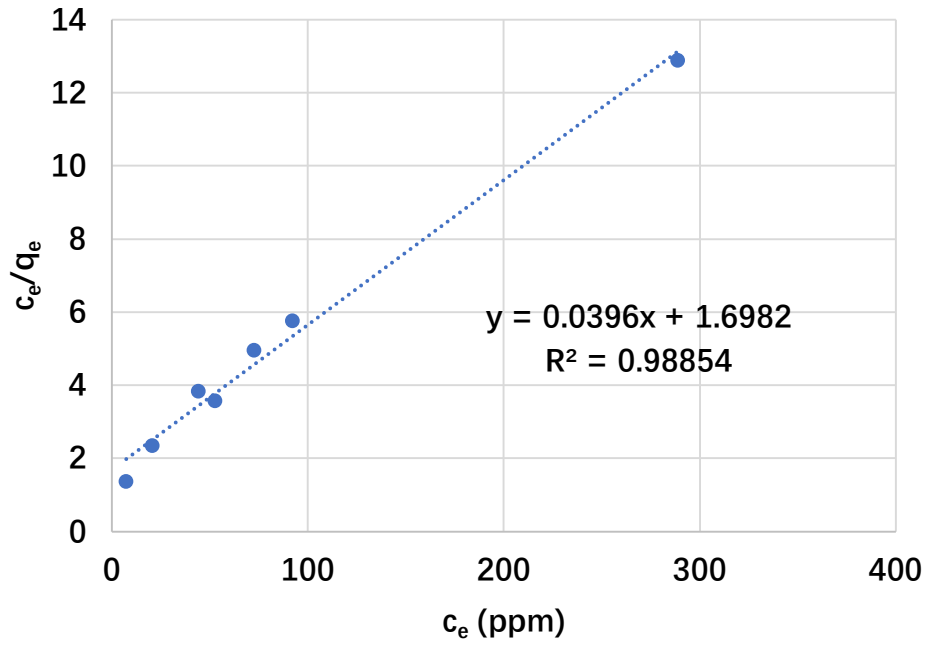

Figure 5-16 Langmuir's isotherm of zinc adsorption by m180AC

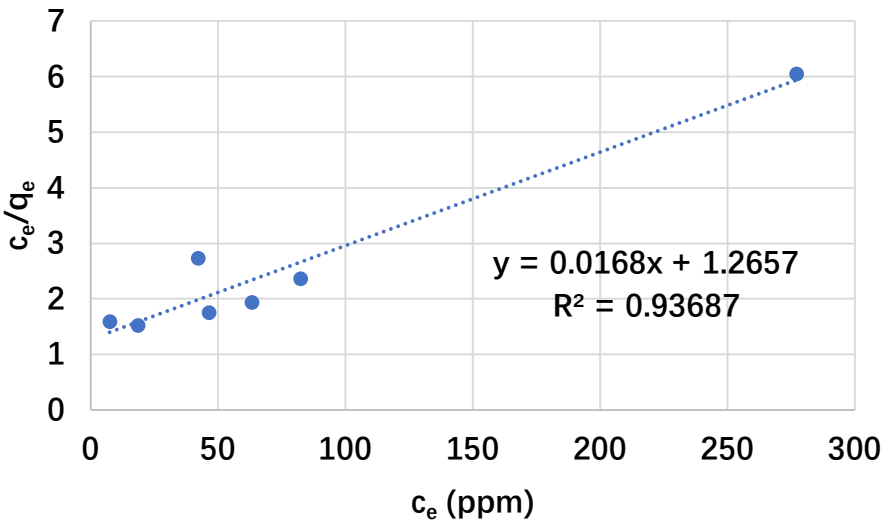

Figure 5-17 Langmuir's isotherm of zinc adsorption by m240AC

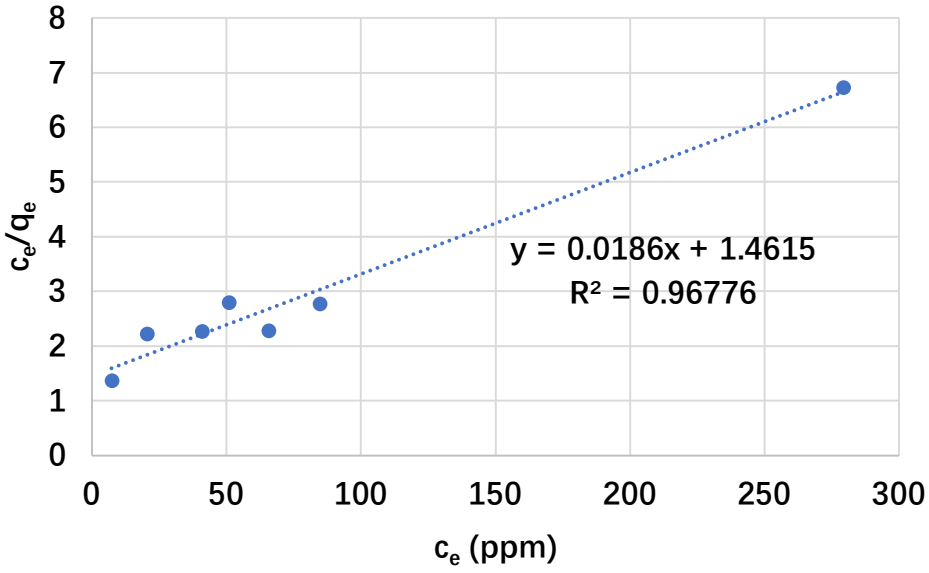

Figure 5-18 Langmuir's isotherm of zinc adsorption by m300AC

The zinc adsorption capacity results from fitting to Langmuir models are shown in Table 5-5.

Table 5-5 Zinc ion adsorption capacity of activated carbons (HNO_3 modified hydrochar samples after KOH activation)

Sample name	Adsorption capacity (mg/g)
m180-AC	25.3
m240-AC	59.5
m300-AC	53.8

The results from Table 5-4 and Table 5-5 are shown in Figure 5-19. From this figure, we can see that activated carbon from HTC temperature at 240℃ (240-AC) showed the highest zinc adsorption capacity among all samples. Meanwhile, HNO_3 assisted HTC process resulted in decrease of zinc adsorption capacity at all HTC temperatures. This is because most of zinc ion in low pH solution (in this experiment, pH=5) are in the form of hydrated zinc ion clusters like $[Zn(H_2O)_6]^{2+}$. These ion clusters are in large size so that they can enter mesopores of activated carbon more easily rather than micropores of activated carbon. The reactive surface chemical property of hydrochar prepared through HNO_3 assisted HTC process made KOH activation process excessively intense so that a large amount of mesepores were destroyed and lowered the zinc adsorption capacity.

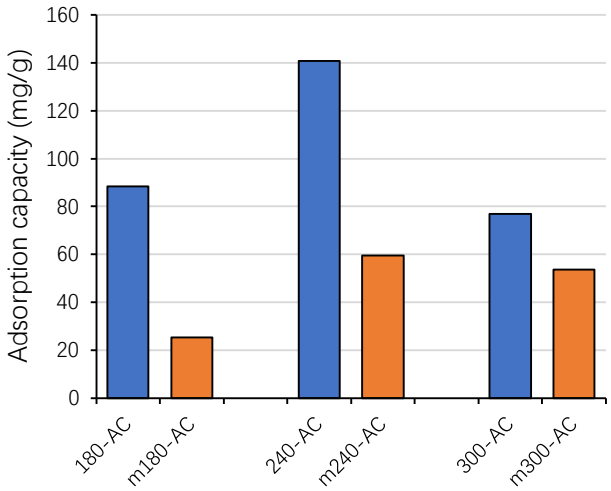

Figure5-19 Zinc ion adsorption capacity of all kind of activated carbons samples

6. Conclusion and recommendation

HTC is a simple, promising conversion technique of converting waste SCG to value-added products. SCG hydrochar utilized as carbonaceous adsorbent and precursor of porous activated carbon was successfully synthesized by HTC in this study.

It was found that hydrothermal treatment operating conditions greatly affected the chemical properties of this kind of SCG hydrochar as well as activated carbon derived from it, thus affected the practical application performance like zinc adsorption in water treatment. In the hydrothermal operating condition under SCG/water ratio of 1:5 and reaction time of 2 h, it was found that 240 ℃ is the most suitable reaction temperature to produce high performance hydrochar adsorbent as well as best precursor for porous activated carbon synthesis. This is because hydrochar synthesized in this temperature obtains more chemically reactive properties such as OFGs than in other reaction temperatures. These OFGs contribute to adsorb heavy metal in the water solution as well as be activated by KOH activation to form developed porous structure.

Meanwhile, activated carbon derived from hydrochar prepared by 5% HNO_3 assist HTC process did not show progress in pore development, which is probably because the reactive surface chemical property of hydrochar prepared through HNO_3 assisted HTC process made KOH activation process excessively intense so that a large amount of mesepores were destroyed.

For the improvement of this research, the following recommendations are suggested.

(1) In the process of KOH activation, adjust the ratio of KOH to SCG hydrochar or activation temperature to control the yield of activated carbon synthesized from HNO_3 modified hydrochar. Because the reaction was intense in the KOH activation conditions mentioned in this thesis.

(2) In the adsorption experiment, we should try tuning the adsorption capacity by changing pH as to gain higher adsorption capacity.

References

[1] Cappelletti S, Piacentino D, Daria P, Sani G, Aromatario M (2015). "Caffeine: cognitive and physical performance enhancer or psychoactive drug". Current Neuropharmacology. **13(1)**: 71–88.

[2] Oder, Tom (2015). "How coffee changed the world". Mother Nature Network. Narrative Content Group.

[3] Ballesteros, L.F., J.A. Teixeira, and S.I.Mussatto (2014). "Chemical, functional, and structural properties of spent coffee grounds and coffee silverskin" Food Bioprocess Technol.**7:3** 493–503.

[4] International Coffee Organization (ICO): http://www.ico.org/prices/new-consumption-table.pdf

[5] Statista Research Department. "Total coffee consumption in Japan 1990-2018" (2020).

[6] National Association of Coffee U.S.A., Inc. "10 Steps from Seed to Cup". (2007).

[7] Ball, Trent; Guenther, Sara; Labrousse, Ken; Wilson, Nikki. "Coffee Roasting". (2007).

[8] Rothstein, Scott. "Brewing Techniques" (2010). The Coffee FAQ.

[9] Ukers, William Harrison. "All about Coffee" (2nd ed. 2010). Gale Research. p. 725.

[10] R.A. Pfluger (1975). "Solid Wastes Origin Collection Processing & Disposal" Soluble Coffee Processing

[11] Supercritical Water Gasification of Biomass: A Literature and Technology Overview.

[12] 平井晴菜, "オスミウム含有廃液処理における超臨界水酸化の適用可能性に関する検討". 東京大学, 修士論文(2018)

[13] Marshall, W.L.; Franck, (1981). "E.U. Ion product of water substance, 0–1000 °C, 1–10,000 bars New International Formulation and its background" J. Phys. Chem. Ref.

[14] Leonel Jorge Ribeiro Nunes, João Paulo Da Silva Catalão (2018), "Advanced Hydrothermal Liquefaction of Biomass for Bio-Oil Production", Torrefaction of Biomass for Energy Applications

[15] Sunil K, Snehalata A (2019). "Current Developments in Biotechnology and Bioengineering" Waste Treatment Processes for Energy Generation P239-258

[16] M.-M. Titirici, M. Antonietti, N. Baccile, (2008) Hydrothermal carbon from biomass: a comparison of the local structure from poly to monosaccharides and pentoses/hexoses, Green Chem. **10** 1204–1212.
[17] A.Jain, R.Balasubramanian, M.P. Srinivasan,(2016) "Hydrothermal conversion of biomass waste to activated carbon with high porosity: A review" Chemical Engineering Journal **283**,789-805
[18] Z. Liu, F.S. Zhang, J. Wu, (2010) "Characterization and application of chars produced from pinewood pyrolysis and hydrothermal treatment", Fuel **89** 510– 514.
[19] Bijoy Biswas, Thallada Bhaskar, (2019) "Advanced Hydrothermal Liquefaction of Biomass for Bio-Oil Production", Biofuels: Alternative Feedstocks and Conversion Processes for the Production of Liquid and Gaseous Biofuels (Second Edition)
[20] O. Bobleter, (1994) "Hydrothermal degradation of polymers derived from plants", Progress in Polymer Science. **19** 797–841.
[21] M.M. Titirici, A. Thomas, S.H. Yu, J.O. Müller, M. Antonietti, (2007) "A direct synthesis of mesoporous carbons with bicontinuous pore morphology from crude plant material by hydrothermal carbonization", Chem. Mater. **19** 4205–4212.
[22] E. Dinjus, A. Kruse, N. Troeger, (2011) "Hydrothermal carbonization–1. Influence of lignin in lignocelluloses", Chem. Eng. Technol. **34** 2037–2043.

[23] S. Kang, X. Li, J. Fan, J. Chang, (2012) "Characterization of hydrochars produced by hydrothermal carbonization of lignin, cellulose, D-xylose, and wood meal", Ind. Eng. Chem. Res. **51** 9023–9031.
[24] C. Falco, N. Baccile, M.-M. Titirici, (2011) "Morphological and structural differences between glucose, cellulose and lignocellulosic biomass derived hydrothermal carbons", Green Chem. **13** 3273–3281.
[25] Daegi Kim, Kwanyong Lee, Daeun Bae, Ki Young Park (2016), "Characterizations of biochar from hydrothermal carbonization of exhausted coffee residue" J Mater Cycles Waste Manag **19** 1036–1043
[26] Kun Zhao, Yeqing Lia, Ying Zhoub, Wenyang Guo, Hao Jiang, Quan Xu (2018), "Characterization of hydrothermal carbonization products (hydrochars and spent liquor) and their biomethane production performance" Bioresource Technology 267 9–16

[27] Z. Liu, F.S. Zhang, (2009) “Removal of lead from water using biochars prepared from hydrothermal liquefaction of biomass”, J. Hazard. Mater. **167** 933–939.
[28] M. Sevilla, A. Fuertes, R. Mokaya, (2011) “High density hydrogen storage in superactivated carbons from hydrothermally carbonized renewable organic materials”, Energy Environ. Sci. **4** 1400–1410.
[29] Dewi Agustina Iryani, Satoshi Kumagai, Moriyasu Nonaka, Keiko Sasaki, Tsuyoshi Hirajima (2017), “Characterization and Production of Solid Biofuel from Sugarcane Bagasse by Hydrothermal Carbonization”, Waste Biomass Valor 8 1941–1951
[30] M. Sevilla, A. Fuertes, (2009) “The production of carbon materials by hydrothermal carbonization of cellulose”, Carbon **47** 2281–2289.
[31] A. Jain, R. Balasubramanian, M.P. Srinivasan, (2015) “Tuning hydrochar properties for enhanced mesopore development in activated carbon by hydrothermal carbonization”, Microporous Mesoporous Mater. **203** 178–185.
[32] C. He, A. Giannis, J.-Y. Wang, (2013) “Conversion of sewage sludge to clean solid fuel using hydrothermal carbonization: hydrochar fuel characteristics and combustion behavior”, Appl. Energy **111** 257–266.
[33] A. Funke, F. Ziegler, (2010) “Hydrothermal carbonization of biomass: a summary and discussion of chemical mechanisms for process engineering”, Biofuels, Bioprod. Biorefin. **4** 160–177.
[34] D. Knezevic, W. Van Swaaij, S. Kersten, (2009) “Hydrothermal conversion of biomass: I, glucose conversion in hot compressed water”, Ind. Eng. Chem. Res. **48** 4731–4743.
[35] M.M. Titirici, R.J. White, C. Falco, M. Sevilla, (2012) “Black perspectives for a green future: hydrothermal carbons for environment protection and energy storage”, Energy Environ. Sci. **5** 6796–6822.
[36] A. Jain, R. Balasubramanian, M. Srinivasan, (2015) “Production of high surface area mesoporous activated carbons from waste biomass using hydrogen peroxide- mediated hydrothermal treatment for adsorption applications”, Chem. Eng. J. **273** 622–629.
[37] C. Falco, J. Marco-Lozar, D. Salinas-Torres, E. Morallon, D. Cazorla-Amoros, M. Titirici, D. Lozano-Castello, (2013) “Tailoring the porosity of chemically activated hydrothermal carbons: influence of the precursor and hydrothermal carbonization temperature”, Carbon **62** 346–355.

[38] A. Romero-Anaya, M. Ouzzine, M. Lillo-Ródenas, A. Linares-Solano (2014), "Spherical carbons: synthesis, characterization and activation processes", Carbon **68** 296–307.
[39] Z. Liu, F.-S. Zhang (2011), "Removal of copper(II) and phenol from aqueous solution using porous carbons derived from hydrothermal chars", Desalination **267** 101–106.
[40] S. Brunauer, P. H. Emmett, and E. Teller (1938), "Adsorption of Gases in Multimolecular Layers," J. Am. Chem. Soc. **60(2)** 309–319.
[41] S.K. Hoekman, A. Broch, C. Robbins (2011) Hydrothermal carbonization (HTC) of lignocellulosic biomass, Energy Fuels **25** 1802–1810.
[42] A. Linares-Solano, D. Lozano-Castello, M. A. Lillo-Ro denas and D. Cazorla-Amoros, (2007) Chemistry and Physics of Carbon, **30**.
[43] Guilherme Nunes Torga, Eduardo Eugênio Spers (2020), "Coffee Consumption and Industry Strategies in Brazil, Chapter 2 - Perspectives of global coffee demand".
[44] G. Myhre, D. Shindell, F.M. Bréon, W.Collins, J. Fuglestvedt, J. Huang, D.Koch, J.F. Lamarque, D. Lee, B.Mendoza, T. Nakajima, A. Robock, G.Ste phens, T. Takemura, H. Zhang (2013), Anthropogenic and natural radiative forcing, Climate change 2013: The physical science basis. Contribution of Working Group I to the Fifth Assessment Report of the Intergovernmental Panel on Climate Change, Cambridge University Press, Cambridge, UK.
[45] Ying Zhang, Xiaolan Song, Yue Xu, Haijing Shen, Xiaodong Kong, Hongmei Xu (2019), "Utilization of wheat bran for producing activated carbon with high specific surface area via NaOH activation using industrial furnace", Journal of Cleaner Production, 210, 366-375.